PNL-6035
UC-70

Nuclear Waste Treatment Program

# Parameters Influencing the Aerosol Capture Performance of the Submerged-Bed Scrubber

C. M. Ruecker
P. A. Scott

April 1987

Prepared for the U.S. Department of Energy
under Contract DE-AC06-76RLO 1830

Pacific Northwest Laboratory
Operated for the U.S. Department of Energy
by Battelle Memorial Institute

Battelle

PNL-6035

## DISCLAIMER

This report was prepared as an account of work sponsored by an agency of the United States Government. Neither the United States Government nor any agency thereof, nor Battelle Memorial Institute, nor any of their employees, makes any warranty, expressed or implied, or assumes any legal liability or responsibility for the accuracy, completeness, or usefulness of any information, apparatus, product, or process disclosed, or represents that its use would not infringe privately owned rights. Reference herein to any specific commercial product, process, or service by trade name, trademark, manufacturer, or otherwise, does not necessarily constitute or imply its endorsement, recommendation, or favoring by the United States Government of any agency thereof, or Battelle Memorial Institute. The views and opinions of authors expressed herein do not necessarly state or reflect those of the United States Government or any agency thereof, or Battelle Memorial Institute.

PACIFIC NORTHWEST LABORATORY
*operated by*
BATTELLE MEMORIAL INSTITUTE
*for the*
UNITED STATES DEPARTMENT OF ENERGY
*under Contract DE-AC06-76RLO 1830*

Printed in the United States of America
Available from
National Technical Information Service
United States Department of Commerce
5285 Port Royal Road
Springfield, Virginia 22161

NTIS Price Codes
Microfiche A01

Printed Copy

| Pages | Price Codes |
|---|---|
| 001-025 | A02 |
| 026-050 | A03 |
| 051-075 | A04 |
| 076-100 | A05 |
| 101-125 | A06 |
| 126-150 | A07 |
| 151-175 | A08 |
| 176-200 | A09 |
| 201-225 | A010 |
| 226-250 | A011 |
| 251-275 | A012 |
| 276-300 | A013 |

3 3679 00052 4019

PNL-6035
UC-70

# PARAMETERS INFLUENCING THE AEROSOL CAPTURE PERFORMANCE OF THE SUBMERGED-BED SCRUBBER

C. M. Ruecker
P. A. Scott

April 1987

Prepared for
the U.S. Department of Energy
under Contract DE-AC06-76RLO 1830

Pacific Northwest Laboratory
Richland, Washington 99352

## SUMMARY

The Submerged-Bed Scrubber (SBS) is a novel air cleaning device that has been investigated by Pacific Northwest Laboratory (PNL) for scrubbing off gases from liquid-fed ceramic melters used to vitrify high-level waste (HLW). The concept for the SBS was originally conceived at Hanford for emergency venting of a reactor containment building. The SBS was adapted for use as a quenching scrubber at PNL because it can cool the hot melter off gas as well as remove over 90% of the airborne particles, thus meeting the minimum particulate decontamination factor (DF) of 10 required of a primary scrubber. The experiments in this study showed that the submicron aerosol DF for the SBS can exceed 100 under certain conditions. A conventional device, the ejector-venturi scrubber (EVS), has been previously used in this application. The EVS also adequately cools the hot gases from the melter while exhibiting aerosol removal DFs in the range of 5 to 30. In addition to achieving higher DFs than the EVS, however, the SBS has the advantage of being a passive system, better suited to the remote environment of an HLW processing system.

The objective of this study was to characterize the performance of the SBS and to improve the aerosol capture efficiency by modifying the operating procedure or the design. A partial factorial experimental matrix was completed to determine the main effects of aerosol solubility, inlet off-gas temperature, inlet off-gas flow rate, steam-to-air ratio, bed diameter and packing diameter on the particulate removal efficiency of the SBS. Several additional experiments were conducted to measure the influence of the inlet aerosol concentration and scrubbing-water concentration on aerosol-removal performance. All of the investigated parameters significantly influenced the performance of the SBS except for the inlet temperature, which had little effect over the 60°-100°C range investigated.

An important parameter influencing aerosol collection efficiency is the diameter of the airborne particulates. Several gas-cleaning devices characteristically exhibit a minimum collection efficiency for particles between 0.1 and 1.0 microns. For the SBS, the minimum was shown to be between 0.3 and 0.7 microns. Thus, all tests in this study were limited to that size range.

The DFs reported in this study therefore represent lower bounds to the DFs that will be encountered for actual melter off gas.

The most influential parameter tested was the flow rate of noncondensible gas. As expected, the percentage of particles penetrating the SBS increases with gas flow rate. The particulate material re-entrained in the off gas also increases with flow rate. The combined influence of increased penetration and increased re-entrainment rapidly decreases the aerosol scrubbing efficiency.

Aerosol solubility directly affects collection efficiency. Water-soluble aerosols are captured much more readily than insoluble aerosols. In this study, typical DFs for sodium chloride (soluble) aerosols were around 100, while DFs for titanium dioxide (insoluble) were generally close to 10. The difference is dominated by the ability of soluble aerosols to quickly penetrate the scrubbing solution/gas interface.

Another important parameter is the steam-to-air ratio. It is well known that steam condensing on aerosols can enhance the capture performance of a particulate filtering device. However, the location of the condensation is important in the case of the SBS. Improvement by a factor of four can be achieved if the steam begins to condense before entering the packed bed. If cooling takes place in the inlet line, the steam condenses on the aerosols, making them effectively larger and easier to capture. Condensation that occurs within the bed takes place mostly at the scrubbing solution/off-gas interface and not on the aerosols. Although the condensing steam results in both diffusiophoretic and thermophoretic deposition on the cold surface, as well as some inertial impaction, the steam is not as useful when condensation occurs at the interface.

The scrubbing efficiency of the SBS increases with increasing aerosol concentration, but the effect is more dramatic with soluble aerosols. The number of collisions increases with concentration as the mean free path decreases, leading to the formation of agglomerates. The particles formed by this process, known as Brownian coagulation, are larger and easier to remove. For insoluble aerosols, the result is a slight increase in efficiency. For soluble aerosols, the outlet concentration is independent of the inlet concentration,

because the aerosols are essentially all captured regardless of the inlet loading. Thus, the DF increases with inlet concentration for both types of aerosols.

The SBS is most effective when the aerosols to be removed are water soluble and the off gas has a high steam-to-air ratio. Melter off-gas streams can be conditioned to meet this case by injecting steam into the off gas. If the off gas is then cooled by a cold vapor injected into the off-gas line at the inlet to the SBS, as noted above, the steam will preferentially condense on the aerosols, and aerosol capture becomes much easier. This concept is used industrially to enhance the collection of aerosols and is known as flux-force/condensation. The condensing steam turns the insoluble aerosols into pseudo-soluble aerosols, because they are pre-wetted by the condensing steam prior to entering the bed. The pre-wetted particles then penetrate the gas/liquid interface more easily and can be absorbed by the scrubbing solution.

Re-entrainment of captured materials can lead to significant reductions in scrubbing performance. For this reason, it is important to minimize the off-gas flow rate and scrubbing solution concentration to limit the number of droplets entrained in the exit off gas, as well as the amount of previously captured material present in each droplet. Re-entrainment losses can also be reduced by adding an appropriate surfactant to the scrubbing solution. The surfactant used in this study was able to essentially eliminate re-entrainment; however, there is currently not enough information to conclude that it will be effective in all cases.

The SBS is a reliable, low-maintenance air-cleaning device that appears to be a strong candidate for the primary scrubber in off-gas systems of high-level waste processing plants. A properly sized and operated SBS has the potential of attaining overall DFs of 100, depending on the characteristics of the off gas. The SBS is also versatile enough to be used for more traditional off-gas cleaning problems. Like other wet scrubbers, the SBS may be especially useful for gas-cleaning applications where the aerosols must be recovered, either to dispose of the material properly or because it has value. Information on sizing an SBS is available in a companion topical report, Design Procedure for Sizing a Submerged-Bed Scrubber for Airborne Particulate Removal, PNL-6036.

## ACKNOWLEDGMENTS

Brent Pulsipher was responsible for deriving the partial factorial test matrix used for this study, as well as performing a statistical analysis of the resulting data. His expertise in these areas is highly appreciated. This document was edited by Sue Liebetrau, whose input has greatly enhanced the report. Tom Powell's assistance during the preparation of experimental apparatus and operation during tests is gratefully acknowledged.

CONTENTS

SUMMARY ..... iii

ACKNOWLEDGMENTS ..... vii

NOMENCLATURE ..... xiii

1.0 INTRODUCTION AND OBJECTIVES ..... 1.1

2.0 AEROSOL PROPERTIES ..... 2.1

2.1 AEROSOL TRANSPORT MECHANISMS ..... 2.1

2.2 AEROSOL CAPTURE MECHANISMS ..... 2.3

2.3 AEROSOL GROWTH BY CONDENSATION ..... 2.5

2.4 AEROSOL GROWTH BY COAGULATION ..... 2.8

3.0 EXPERIMENTAL EQUIPMENT ..... 3.1

3.1 OFF-GAS CLEANING SYSTEM ..... 3.2

3.2 SUBMERGED-BED SCRUBBER ..... 3.3

3.3 AEROSOL GENERATOR ..... 3.3

3.4 ANALYTICAL PARTICLE-SIZING EQUIPMENT ..... 3.5

4.0 EXPERIMENTAL DESIGN ..... 4.1

4.1 OFF-GAS MAKEUP ..... 4.1

4.2 SBS OPERATION ..... 4.1

4.3 OFF-GAS SAMPLING ..... 4.2

4.4 CSAS CALIBRATION ..... 4.2

4.5 EXPERIMENTAL MATRIX ..... 4.3

5.0 INFLUENCE OF VARIOUS PARAMETERS ON THE AEROSOL CAPTURE PERFORMANCE ..... 5.1

5.1 SIMULATION OF IMPORTANT COMPOUNDS IN LFCM OFF GAS ..... 5.2

5.2 INLET AEROSOL CONCENTRATION ..... 5.5

5.3 HUMIDITY ..... 5.7

5.4 BED DIAMETER ..... 5.10

5.5 PACKING SIZE ..... 5.13

5.6 INLET TEMPERATURE ..... 5.15

5.7 EFFECT OF SUB-DEW-POINT INLET CONDITIONS ..... 5.20

5.8 RE-ENTRAINMENT ..... 5.21

6.0 CONCLUSIONS AND RECOMMENDATIONS..... 6.1

6.1 INFLUENCE OF INVESTIGATED PARAMETERS ..... 6.1

6.1.1 Process Variables ..... 6.1

6.1.2 Design Variables ..... 6.3

6.1.3 Operating Variables ..... 6.4

6.2 EXPECTED INFLUENCE OF SOME ADDITIONAL PARAMETERS ..... 6.4

7.0 REFERENCES ..... 7.1

APPENDIX ..... A.1

## FIGURES


1 Operating Principles of the Submerged-Bed Scrubber ..... 1.2

2 Classical Aerosol Capture Mechanisms ..... 2.3

3 Pilot-Scale Off-Gas System ..... 3.1

4 Cross-Sectional View of the Submerged-Bed Scrubber ..... 3.4

5 Influence of Inlet Concentration on SBS Performance ..... 5.6

6 Influence of Steam on SBS Performance ($TiO_2$) ..... 5.8

7 Influence of Steam on SBS Performance (NaCl) ..... 5.10

8 Influence of Bed Diameter on SBS Performance ..... 5.11

9 Predicted Interaction Between Bed Diameter and Steam-to-Air Ratio at a Superficial Velocity of 0.3 m/s ..... 5.13

10 Collection Efficiency as a Function of Particle Diameter ..... 5.14

11 Influence of Packing Size on SBS Performance ..... 5.16

12 Typical Axial Bed Temperature Profile ..... 5.18

13 Outlet Concentration Due to Re-Entrainment as a Function of Time .... 5.23

14 Effect of Scrubbing-Solution Concentration on Re-Entrainment ..... 5.24

15 Particle Size Distribution of Titanium Dioxide Suspended in the Scrubbing Water ..... 5.25

16 Effect of Gas Velocity on Re-Entrainment ..... 5.27

17 Effect of Dow Defoamer DB-110A on Re-Entrainment ..... 5.29

## TABLES


1 Typical Brownian Coagulation Rates ..... 2.9

2 SG 40 Particle Size Distribution for DOP ..... 3.5

3 Values for Experimental Parameters ..... 4.3

4 Parameter Estimates ..... 5.2

5 Influence of Aerosol on SBS Performance ..... 5.3

6 Experiments Conducted at Inlet Temperatures Below the Dew Point .... 5.20

A.1 0.5-m-Diameter Bed with 1-cm Packing ..... A.1

A.2 0.4-m-Diameter Bed with 1-cm Packing ..... A.2

A.3 0.4-m-Diameter Bed with 0.3-cm Packing ..... A.3

A.4 0.5-m-Diameter Bed with 0.3-cm Packing ..... A.4

A.5 0.5-m-Diameter Bed with 1-cm Packing ..... A.5

A.6 0.4-m-Diameter Bed with 1-cm Packing ..... A.7

A.7 0.4-m-Diameter Bed with 0.3-cm Packing ..... A.8

A.8 0.5-m-Diameter Bed with 0.3-cm Packing ..... A.9

## NOMENCLATURE

| | |
|---|---|
| $C$ | Aerosol Concentration, particles/cc |
| $D$ | Bed Diameter, m |
| $d$ | Particle Diameter, cm |
| DF | Decontamination Factor, defined as the aerosol mass flow rate in divided by the mass flow rate out, dimensionless |
| $F$ | Superficial Velocity, m/s |
| $k$ | Coagulation Constant, $cm^3$/particles•s |
| $k_B$ | Boltzman Constant, erg/molecule•K |
| $M$ | Molecular Weight, g/gmol |
| $m$ | Aerosol Mass Flow Rate, g/s |
| $N$ | Avogadro's Number, molecules/mol |
| $n_i$ | Moles of Component i, mol |
| $P$ | Packing Diameter, cm |
| $p$ | Probability that a Value for a Coefficient is Not Significantly Different than Zero (t-Test), fractional percent |
| $p_{AO}$ | Vapor Pressure of the Solvent in Equilibrium with a Droplet, dyne/$cm^2$ |
| $p_{AS}$ | Vapor Pressure of Pure Solvent at T, dyne/$cm^2$ |
| $p_o$ | Vapor Pressure in Equilibrium with a Flat Liquid Surface, dyne/$cm^2$ |
| $p_s$ | Vapor Pressure in Equilibrium with a Pure Liquid Droplet, dyne/$cm^2$ |
| $R$ | Gas Constant = $8.314 \times 10^{-7}$ erg/gmol•K |
| $S$ | Supersaturation Ratio, dimensionless |
| $T$ | Temperature, K |
| $t$ | Time, s |
| $\bar{v}_i$ | Molar Volume of Component i, $cm^3$/molecule |

Greek

| | |
|---|---|
| $\alpha$ | Volumetric Steam-to-Air Ratio, dimensionless |
| $\beta$ | Coefficient or Parameter Estimate in Equation 1, units depend on multiplier (see Table 3) |
| $\rho_L$ | Liquid Density, g/$cm^3$ |
| $\sigma$ | Surface Tension, dyne/cm |

# 1.0 INTRODUCTION AND OBJECTIVES

Vitrification using a liquid-fed ceramic melter (LFCM) has been selected in the United States as the reference process for immobilization of high-level radioactive waste currently stored at the Hanford, Savannah River and West Valley sites. Some compounds present in the liquid high-level waste (HLW) are volatile at melter operating temperatures and are vented in an off-gas line. The off gas also includes volatile constituents like water vapor, nitrogen oxides, and halogen gases, as well as entrained HLW feed. Off gas drawn from the melter must be cleaned before being vented to the atmosphere. Unfortunately, some of the radioactive compounds volatilized in the melter condense in the off-gas piping and form aerosol particles that are difficult to capture (Goles and Sevigny 1983).

Because off gas exiting the LFCM is highly radioactive, the first treatment stages must be located in a remote area. Consequently, it is desirable that the first scrubber be highly reliable with minimum maintenance. This constraint led to the investigation and testing of the submerged-bed scrubber (SBS), as part of the U.S. Department of Energy's Nuclear Waste Treatment Program, to determine how the performance can be made most effective for this application.

The SBS is a passive aqueous scrubber that can be used as a primary gas cleaning device, which must be able to achieve a minimum particulate DF of 10 (Gurley et al. 1986) as well as to quench the off gas. The concept for the SBS was originally developed at Hanford for capture of aerosols during an emergency vent of a reactor containment building (Hilliard, McCormack and Postma 1981). Pacific Northwest Laboratory modified the design for use in melter off-gas treatment (Siemens et al. 1986), and has tested it since 1983. The operating principles of the SBS are illustrated in Figure 1. The device consists of a fixed bed submerged in an aqueous pool. The off gas is introduced at the bottom of the packing and is allowed to bubble up through the bed. The apparent density of the two-phase fluid flowing up through the bed is less than the density of the water surrounding the bed. This difference in densities causes a natural pumping action, as hydrostatic pressure forces the surrounding water up

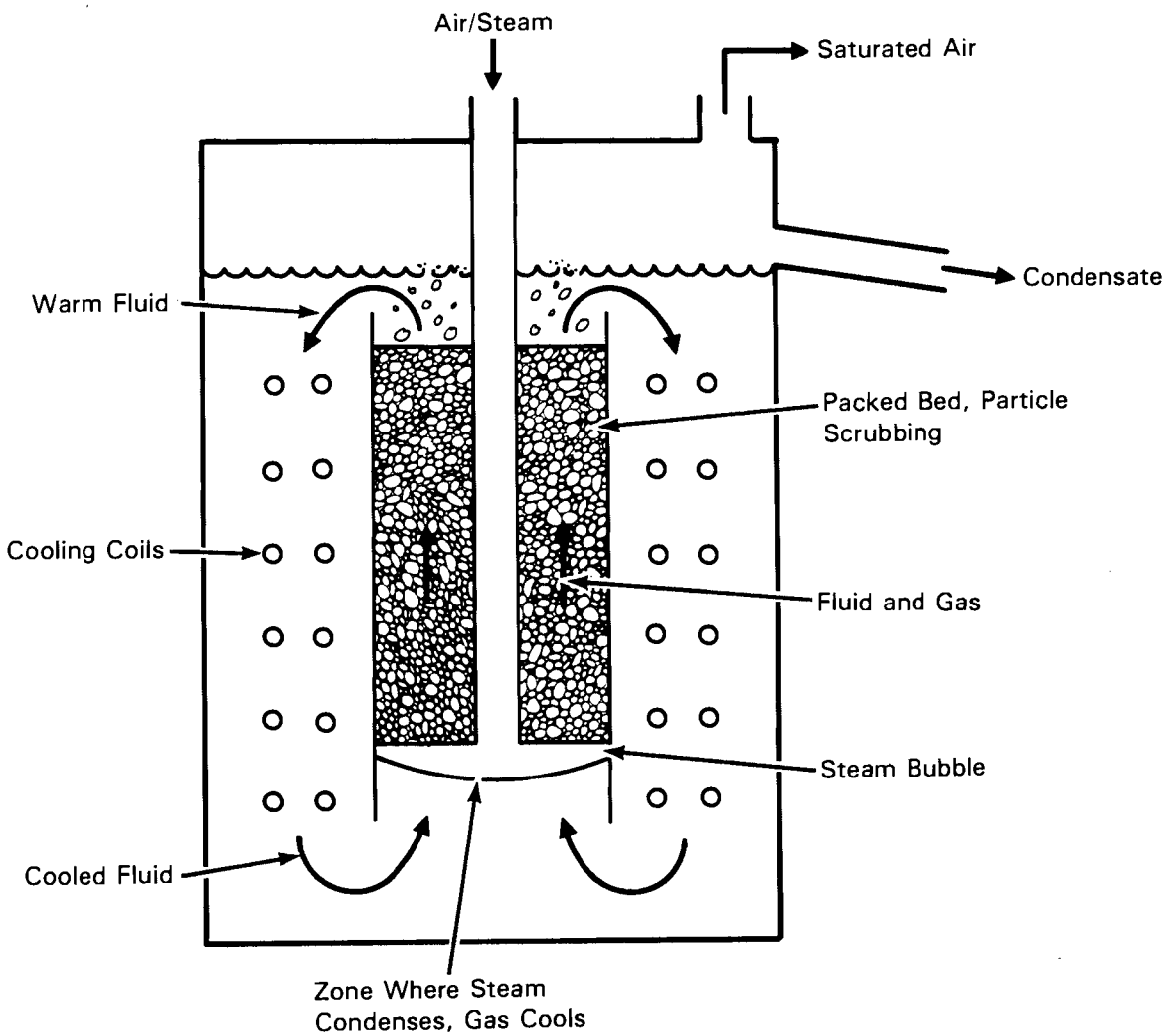


FIGURE 1. Operating Principles of the Submerged-Bed Scrubber

through the bed. The pumping action helps to keep the bed from plugging with captured particulate material and improves the heat removal by the cooling coils.

The SBS contains no moving parts, so it is ideal for use in a remote location. However, its development has been so recent, it has yet to be fully characterized. A better understanding of the SBS was necessary to determine whether possible design modifications or operating changes could be implemented in the existing design to achieve better aerosol removal efficiencies than previously reported (Scott, Goles and Peters 1985). The objective of this study

was to determine the optimum operating conditions by investigating the parameters affecting the performance of the SBS. These results were used as a design basis in a companion topical report that demonstrates proper sizing of an SBS (Ruecker and Scott 1986).

# 2.0 AEROSOL PROPERTIES

An aerosol is defined as a liquid or solid particle that is suspended in a gas. Aerosol particles range in size from 0.001 to 100 microns and can remain suspended for as little as a few seconds or as long as a few years. Although the particles are highly mobile, they tend to attach themselves to most surfaces upon contact, making it possible to remove them from a gas by providing such a surface. The main bonding forces are London van der Waal forces, electrostatic forces, and the surface tension of absorbed liquid films. Of these, the London van der Waal forces are the most prominent (Hinds 1982). These forces arise because the random movement of electrons in any material creates momentary areas of charge concentration called dipoles. At any instant, these dipoles induce complementary dipoles in neighboring material, which give rise to attractive forces. These forces decrease rapidly with separation distance between surfaces.

## 2.1 AEROSOL TRANSPORT MECHANISMS

Aerosols can be transported to a surface by several mechanisms. The main transport mechanism is usually convection. Aerosol particles are easily carried along by the off gas because of their small size and light weight. Next to convection, diffusion is the primary transport mechanism for particles less than 0.1 micron in size. Other transport mechanisms include thermophoresis, photophoresis, Stephan flow and flow due to radiant pressure. All of these forces are very weak but can cause aerosol motion because of the low inertia of the particles. Transport due to radiant pressure and photophoresis is not important for the SBS but is included for completeness. A more thorough treatment of aerosol transport mechanisms is presented by both Hidy (1984) and Hesketh (1986).

Thermophoresis. Small particles are constantly being bombarded by gas molecules. When a particle is in a temperature gradient, it will feel a greater momentum transfer from the gas molecules on the hot side of the particle than it will on the cold side. The difference in momentum transfer results in a net movement away from the heat source. The thermophoretic velocity of

0.1-micron particles, for example, exceeds the terminal settling velocity, even for weak temperature gradients (1°C/cm). It is likely that thermophoresis contributes to the collection of fine particles in air cleaners in which hot gas streams are cooled.

Photophoresis. Photophoresis is a special case of thermophoresis in which illumination of the particle causes a temperature gradient inside the particle. Heat is transferred from the particle to the surrounding gas at different rates, resulting in an induced temperature gradient. The actual transport phenomenon is the same as for thermophoresis, but the temperature gradient in the gas is induced by heat transferred from the particle. The aerosols, again, will move down the temperature gradient resulting in the transport of aerosols away from the source of illumination.

Radiation Pressure. The force of radiant pressure is a result of momentum transfer, not from gas molecules but from the deflection and absorption of light. The light can be thought of as a stream of photons whose momentum is altered as they are deflected (or absorbed) by the particle so as to cause a force away from the light.

Brownian Diffusion. Small particles will follow an irregular path caused by the random variations in the collisions with gas molecules. The resulting transfer of momentum causes the aerosol particles to change direction. Brownian diffusion is an important transport mechanism for submicron particles and is largely responsible for the capture of particles less than 0.1 micron in situations where transport distances are small and collection times are large.

Diffusiophoretic Force. Concentration gradients result in the diffusion of molecules along the gradient. If the diffusing molecules are of different weights, a force will be felt by any aerosol present in the concentration gradient. This force is due to unequal momentum transfer from the diffusing molecules. The net movement of the aerosol will be along the concentration gradient; the direction of transport will depend on the nature of the diffusing molecules. This transport mechanism is related to Brownian diffusion but is generally not as important.

Stephan Flow. Near evaporating or condensing surfaces, an aerodynamic flow of air exerts Stokes drag on a particle. This flow is directed away from evaporating surfaces and towards condensing surfaces. In order to maintain constant total pressure in the vicinity of an evaporating surface, the concentration gradient of vapor must be balanced by an equal and opposite concentration gradient of air. The combination of diffusiophoresis and Stephan flow is exploited in venturi scrubbers, where supersaturated conditions are established that cause condensation and Stephan flow to carry fine particles onto condensing droplets and surfaces.

## 2.2 AEROSOL CAPTURE MECHANISMS

Aerosols can be brought into the vicinity of a collecting medium by any combination of the previously mentioned transport mechanisms. Once the particle is near the collecting surface, there are several methods by which it can be captured. The more traditional mechanisms are shown in Figure 2 for flow around a cylindrical fiber or spherical packing. The likelihood of a particle's being captured by a given mechanism is directly related to the size of the particle. A review of the more important capture mechanisms is given below. A more detailed discussion is presented by Hinds (1982).

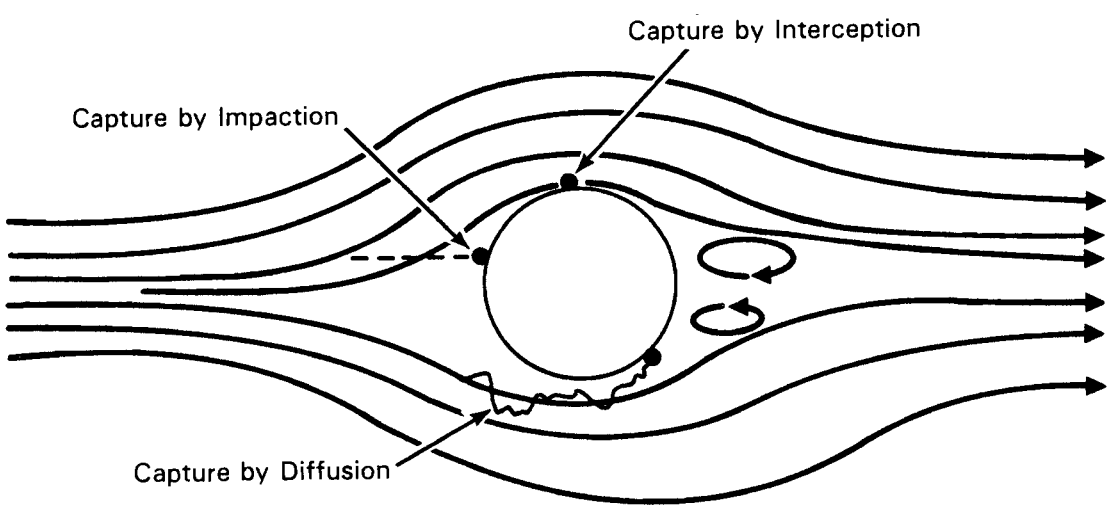


FIGURE 2. Classical Aerosol Capture Mechanisms

Interception. An aerosol can be removed from an air stream when the gas streamline it is following comes within one particle radius of the surface of the collecting medium. For pure interception, it is assumed that particles follow the streamlines perfectly, that they have negligible inertia or Brownian motion. The collection efficiency due to interception increases as the ratio of the particle's diameter to the diameter of the collecting medium increases. The minimum efficiency particle diameter for a given filter is usually between 0.1 and 1 micron (Hinds 1982; Shaw 1978; McCarthy et al. 1976). Aerosols in this size range are too small to be captured by inertial impaction and too large to be significantly influenced by Brownian motion. Thus, interception is the only effective capture mechanism. Larger and small particles have higher overall capture efficiencies because of contributions from impaction and diffusion. Interception is probably the only mechanism that does not depend on the flow rate of the gas stream.

Inertial Impaction. Particles are captured by impaction when their own momentum prevents them from following a streamline around an obstruction. The inertia of the particles causes them to collide with the object, which results in their removal from the gas stream. This mechanism is more important for larger particles, and the efficiency increases with gas flow rate because it increases the momentum of the aerosols.

Brownian Motion. The path of a small particle is affected by Brownian motion, which causes the particle to follow an irregular path. This motion increases the probability that the particle will hit the surface of a collecting medium while traveling past on a nonintercepting streamline. This mechanism is largely responsible for the removal of particles of less than 0.1 micron. Because Brownian motion is not related to the inertia of the fluid, this capture mechanism is improved with longer residence time (low velocity).

Gravitational Settling. The force of gravity will eventually cause aerosols to fall out of a stagnant gas. Particles can be removed from a gas stream by this mechanism if they are large enough and the gas flow rate is low enough.

Electrostatic Attraction. Aerosol particles are capable of carrying a charge, so they may be exposed to electrostatic attractions. A charged

particle will be attracted to a collection medium of opposite charge and will migrate in that direction. This capture mechanism is used in electrostatic precipitators to remove aerosols from gas streams (White 1963). The attractive forces can be very large and collection efficiencies very high, but there is a cost incurred in charging the particles as they enter the precipitator, and a problem in removing the particles from the collecting medium without causing them to be re-entrained.

## 2.3 AEROSOL GROWTH BY CONDENSATION

As was noted in the previous section, the ease with which a particle is removed from a gas stream is a function of the size of the particle. In general, particles less than 0.01 μm are effectively removed using high-efficiency filters as a result of Brownian motion (Hinds 1982), whereas particles larger than 10 μm are easily removed by a simple spray chamber (Schifftner and Hesketh 1986). Particles in the intermediate range can be collected, but not so easily. Therefore, it is sometimes desirable to shift the particle size distribution into a region where the aerosols are removed more efficiently.

One means of increasing the size distribution of particles entering an aerosol filtering device is to condense a vapor on the particles. The added volume of the condensing vapor will increase the effective diameter of the aerosols, thus shifting the size distribution toward larger diameters where the particles can be efficiently removed. This concept has been proven to be an effective means of enhancing the aerosol collection efficiency by Calvert and Gandhi (1977), who used steam as the condensible vapor.

The growth of particles in the presence of condensible vapors can be achieved by several means: 1) an adiabatic expansion of a gas; 2) the mixing of a warm, moist gas with a cool gas stream; or 3) cooling of a moist gas through a heat transfer surface. In the absence of aerosols, a supersaturated vapor condenses by homogeneous nucleation on molecular clusters. If aerosols are present, they can act as nuclei for heterogeneous condensation. The discussion of homogeneous nucleation that follows provides an appropriate introduction to particulate growth by condensation.

Homogeneous Nucleation. Whether or not a vapor will condense on a pure liquid of the same species is a function of the size of the droplet and the supersaturation ratio S, which is defined as the vapor pressure $p_s$ in equilibrium with a pure liquid droplet divided by the equilibrium vapor pressure $p_o$ over a flat liquid surface of the same species.

$$S = p_s/p_o \tag{1}$$

The supersaturation ratio necessary before condensation will occur on a pure liquid droplet of a given diameter can be determined from the Kelvin Equation, as discussed by Calvert and Englund (1984):

$$\ln S = \frac{4\sigma M}{RT\rho_L d} \tag{2}$$

where d = the diameter of the droplet, cm

M = molecular weight, g/gmol

$\sigma$ = the surface tension of the liquid, dyne/cm

$\rho_L$ = the density of the pure liquid, $g/cm^3$

The Kelvin Equation shows that the supersaturation ratio necessary for a vapor to condense on a given droplet is a decreasing function of the diameter of the droplet. At very large diameters the supersaturation ratio necessary for condensation to occur approaches 1.0. On the other hand, as the droplet size decreases, the supersaturation ratio necessary for condensation becomes increasingly larger. The Kelvin Equation implies that if there were no liquid droplets present in the supersaturated vapor, the supersaturation ratio would have to be infinite before homogeneous nucleation would occur. This equation helps to explain why vapors tend to condense on foreign nuclei as opposed to undergoing homogeneous nucleation. In reality, as the supersaturation ratio increases, the random accumulations of molecular clusters begin to be sufficient to act as condensation nuclei. The existence of these clusters has been experimentally verified by Miller and Kusch (1956). The point at which the supersaturation ratio is high enough for the molecular clusters to form is significantly higher than would have been necessary for condensation to occur had

there been condensation nuclei. Vapors generally do not reach significant rates of self-nucleation until saturation conditions exceed 200 to 400%.

Heterogeneous Condensation. The presence of foreign nuclei, or aerosols, in a condensible vapor system will greatly change the supersaturation ratio necessary to achieve condensation. The actual supersaturation ratio required to initiate condensation, known as the critical supersaturation ratio, is a function of several variables: the size, surface structure, wettability, solubility and electrical charge of the condensation nuclei. Thus, it is very difficult to predict the critical supersaturation ratio.

The importance of wettability of the nuclei by the condensing vapor was demonstrated in a theoretical development of the free energy of condensation for vapors on foreign nuclei by Fletcher (1958). The ratio of the drop radius to the particle radius was also an important parameter in the theoretical equation. This work was limited to condensation on insoluble spherical particles. Consideration of soluble nuclei is complicated by the dissolution process. As a small salt particle is exposed to increasing relative humidity, it will remain solid up to a characteristic relative humidity less than 100%, where it will absorb water and dissolve to form an aqueous solution. Examples of relative humidities less than 100% that still result in the dissolution of large salt crystals are given by Hidy (1984), based on the results of Stokes and Robinson (1949), Dean (1973), and Friedlander (1977).

The value of the relative humidity where condensation occurs depends on the size of the salt particle as a result of the Kelvin effect. Hidy (1984) presents a theoretical example demonstrating the effect of a solute, such as sodium chloride or ammonium sulfate, on the supersaturation ratio of a vapor in equilibrium with a droplet of a given size. For a dilute binary system, the Kelvin Equation becomes

$$\ln \frac{p_{AS}}{p_{AO}} = \frac{4\sigma\bar{v}_A}{dNk_BT} - \frac{24n_B\bar{v}_B}{4\pi d^3} \qquad (3)$$

where $p_{AO}$ = vapor pressure of the pure solvent at T, dyne/cm$^2$

$p_{AS}$ = vapor pressure of the solvent in equilibrium with the droplet, dyne/cm$^2$

$\bar{v}$ = molar volume of the solvent (A) and solute (B), cm$^3$/molecule

At large diameters, the influence of a fixed amount of solute will become insignificant, and Equation 3 will reduce to that of the Kelvin Equation for a single component system. However, as the droplet diameter decreases, the solute has an increasing effect on the supersaturation ratio necessary to maintain a stable droplet size. For a pure liquid, the supersaturation ratio will continue to increase as the droplet size decreases (Equation 2). For a binary system, the supersaturation ratio will start to decrease with decreasing droplet size as the result of the $d^{-3}$ term in Equation 3. The equilibrium saturation ratio will actually fall below one as the percentage of solute in the droplet continues to increase. This theoretically predicted result is consistent with the experimental results previously mentioned of salt crystals dissolving at relative humidities less than 100%.

Once a droplet of critical size has been nucleated, it will continue to grow. The rate at which the particle grows is a function of the vapor pressure in the gas phase and the conditions at the droplet's surface. For the purposes of this study, it is sufficient to say that the rates of condensation are fast enough that a theoretical discussion of the subject is unnecessary. Information on the subject of condensation growth rates is available elsewhere (Calvert and Englund 1984; Hidy 1984).

## 2.4 AEROSOL GROWTH BY COAGULATION

Coagulation occurs when aerosols come in contact and coalesce or adhere to each other. The process of coagulation can be very beneficial during attempts to remove particles from a gas stream. Not only will coagulation reduce the total number of particles in the gas stream, it will also increase their distribution toward larger diameters, making them easier to capture. This concept has been taken to extremes through the use of acoustical energy to dramatically increase the coagulation rate, which leads to extremely large particles that can be removed from a gas stream with a simple device such as a cyclone (Danser

and Neuman 1949; Boucher 1961). Particle growth from 0.5 μm to 100 μm using acoustical agglomeration techniques has been achieved by St. Clair (1949). The rate of coagulation does not necessarily need to be enhanced by acoustics to be important; significant coagulation can occur in a turbulent gas stream as well as in still air.

Brownian Coagulation. The random motion of aerosols due to Brownian motion is responsible for the majority of collisions between particles, which result in coagulation. The coagulation rate of many aerosols has been found to follow a very simple rate expression:

$$\frac{dC}{dt} = -kC^2 \tag{4}$$

where $k$ = coagulation constant, $cm^3$/particles•s
$C$ = particle concentration, particles/$cm^3$

Experimental coagulation constants measured for various aerosols by Green and Lane (1964) were generally on the order of $5 \times 10^{-10}$ $cm^3$/particles•s. This number can be used to estimate the time required for the aerosol concentration to be decreased by a factor of two for a given initial concentration (Table 1).

Because the rate of Brownian coagulation depends on particle concentration, higher concentrations will coagulate more quickly. Thus, all dense clouds of particles will have approximately the same concentrations within about one minute following their creation, regardless of their initial concentrations.

Studies investigating the effect of particle charge on the rate of coagulation have had mixed results. Early experiments showed no effect of charge on

TABLE 1. Typical Brownian Coagulation Rates

| Initial Concentration (particles/$cm^3$) | $t_{1/2}$ |
|---|---|
| $10^{11}$ | 0.02 s |
| $10^9$ | 2.0 s |
| $10^6$ | 33.3 min |

coagulation rates for particles in the micron to submicron size range. A later study (Gillespie 1953) showed coagulation rates to be increased by an order of magnitude as a result of charge. In a carefully designed experiment involving dioctylphthalate aerosols of approximately 1.5 μm, Devir (1967) was able to verify the earlier findings that charge had little effect on the rate of coagulation.

Coagulation in Laminar Flow. In laminar flow, particles can collide and agglomerate as a result of differences in the velocity at which they are traveling. The laminar flow coagulation rate, neglecting Brownian coagulation, is a function of the cube of the particle radius and the fluid velocity gradient; thus, small changes in the particle size have a large effect on the required velocity gradient. The particle coagulation rate due to laminar flow is described by Hidy (1984). The relative importance of laminar flow coagulation compared to Brownian coagulation is addressed by Calvert and Englund (1984). Coagulation due to laminar flow inside the SBS is not expected to be an important process and will therefore not be described further.

Coagulation in Turbulent Flow. Collisions between aerosols leading to coagulation can result from two different mechanisms in turbulent flow. Spatial variations in the gas velocity result in neighboring particles having different velocities, which can lead to collisions. Because each particle is moving relative to the surrounding air as a result of inertia, particles of unequal size travel at different velocities, which can also lead to collisions. Saffman and Turner (1956) showed that the collision rate of water droplets in clouds due to differences in the particles' inertia can be the dominant mechanism for coagulation in turbulent flow.

Knowledge of the fundamental aerosol transport, capture, condensation, and coagulation mechanisms is necessary to explain how various parameters influence the aerosol-scrubbing performance of the SBS. Knowledge of the fundamental mechanisms can also lead to a better understanding of which parameters are likely to influence the performance of the SBS and what modifications may improve the aerosol removal performance.

## 3.0 EXPERIMENTAL EQUIPMENT

The submerged-bed scrubber used in this study was part of an existing off-gas system for a pilot scale liquid-fed ceramic melter located on the Hanford Site. A schematic of the portion of the off-gas system used is shown in Figure 3. The system was constructed almost entirely of stainless steel. Four-inch (0.1-m) schedule 10S piping was used in all cases except for the inlet

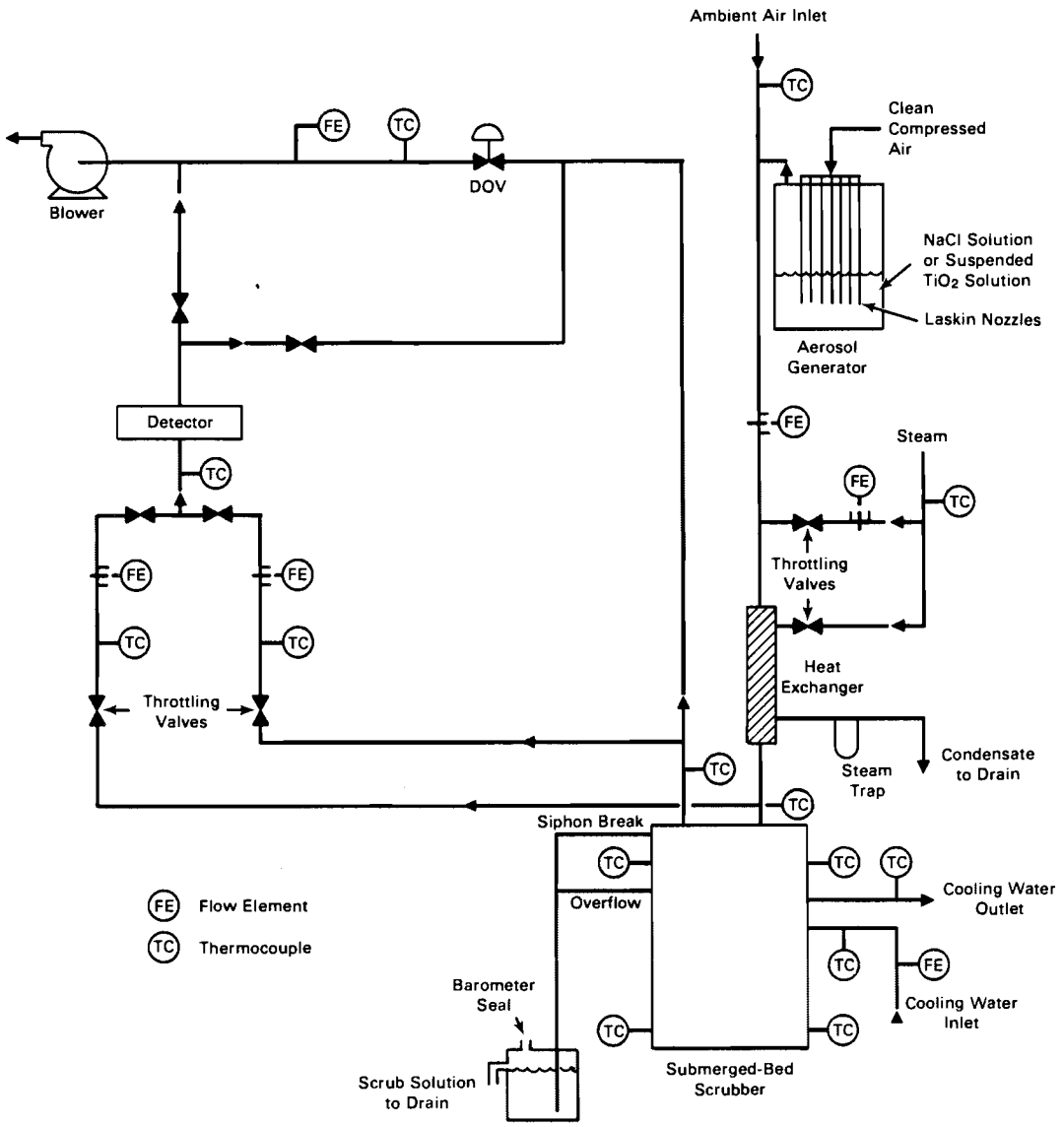


FIGURE 3. Pilot-Scale Off-Gas System

line to the SBS, which was 3 inches (7.6 cm SCHD 10S) and the sample lines, which were 1 inch (2.54 cm SCHD 40). The equipment relevant to this study included the aerosol generator, the analytical equipment used to determine the size and concentration of particles present in the off gas, the SBS and the associated off-gas system.

## 3.1 OFF-GAS CLEANING SYSTEM

A blower generated the suction necessary to induce flow through the system. Variable off-gas flow rates were achieved by adjusting a diaphragm-operated valve (DOV). Particulate material in the off gas was produced by an aerosol generator. It was necessary to combine the output from the aerosol generator with room air to establish the necessary volumetric flow rates. Steam was injected into the off gas during some experiments, to raise the humidity. The off gas passed through a tube-and-shell heat exchanger before entering the SBS. Steam was used on the shell side to raise the inlet temperature. A high-efficiency mist eliminator (not shown) was used down stream of the SBS to remove any aerosols not captured by the SBS before the off gas was vented to a stack.

The exit off-gas flow rate was measured with a PSE series 100 flow sensor which is a velocity head type of element. The inlet air flow rate and steam injection rate were determined independently by orifice plates. Differential pressure transducers indicated the pressure drops across all flow elements and major system components. Output signals from the transducers were transmitted to a signal conditioner where they were converted to pressure drops and flow rates. Data were transferred from the signal conditioner to a Hewlett Packard 9836C computer at a scan rate of 10 seconds. Values were averaged over a 2-minute period, and the resulting mean value was stored on a hard disk. Temperature measurements were also scanned every 10 seconds with the use of a data acquisition system. Mean temperature values were also calculated every 2 minutes and recorded on the disk. Type K thermocouples were used for all temperature measurements. Thermocouple locations can be found on Figure 3.

## 3.2 SUBMERGED-BED SCRUBBER

The SBS consisted of a bed of ceramic spheres submerged in a stainless steel tank 1.68 m x 0.91 m in diameter. A cross-sectional view of the SBS is shown in Figure 4. The bed was contained in a 0.96-m section of 0.51-m-diameter pipe. Two concentric cooling coils circled the bed in the annular space between the pipe and the tank wall.

The pipe was filled with Norton Denstone® 57 ceramic spheres. Both 0.3-cm and 1-cm spheres were investigated. A stainless steel screen with radial reinforcement bars supported the bed. A second screen was welded in place on top of the packing to prevent the bed from fluidizing. The support plate was located 0.23 m from the bottom of the pipe, thus allowing room for a gas bubble to form under the packing. This skirt prevented the off gas from migrating radially out past the edge of the bed. Two concentric pipes ran through the center of the bed. The off gas entered the SBS through the inner pipe. Premature heat transfer from the off gas to the scrubbing solution was prevented by packing the void space between the two pipes with insulation.

Thermocouples were located in the inlet and outlet off-gas lines, as well as at the outlets of the two cooling coils. A thermocouple located at the inlet of coil #2 measured the inlet water temperature. This temperature was also used as the inlet temperature for coil #1 and the SBS make-up water temperature, because all three lines originated from the same source. Thermocouples located below coil #1 and above coil #2 measured the temperature of the scrubbing solution.

## 3.3 AEROSOL GENERATOR

A Virtis SG 40 smoke generator was used to create the off gas. The reservoir in the generator was filled with either a soluble or insoluble compound and purified water. Filtered-compressed air entered the generator through any combination of one to six Laskin-type nozzles. The air stream leaving the nozzle sheared the liquid in the reservoir, producing predominately submicron aerosols. Table 2 shows the size distribution produced by the generator, as

---

® Registered trademark of Norton Chemical Process Products, Akron, Ohio.

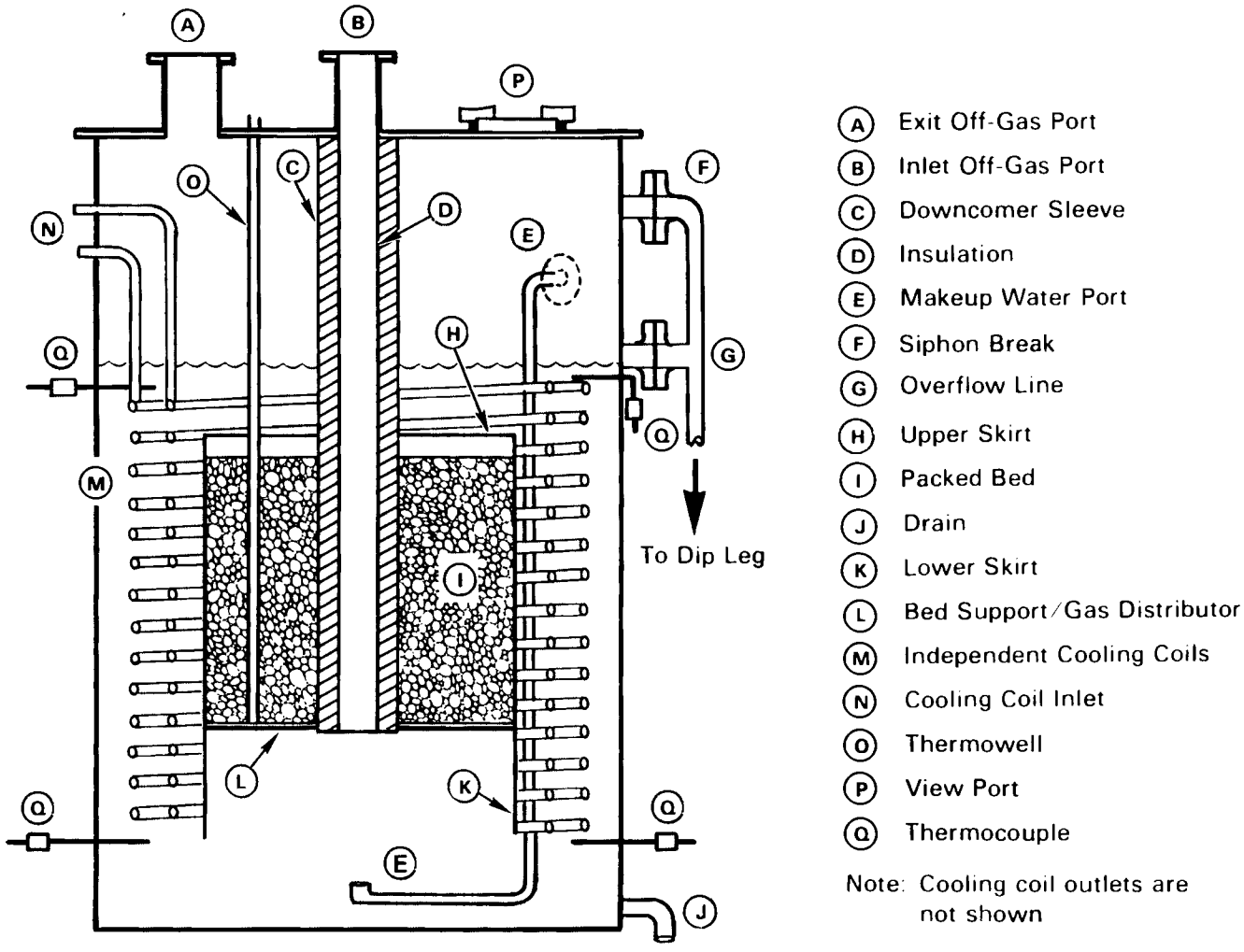


FIGURE 4. Cross-Sectional View of the Submerged-Bed Scrubber

TABLE 2. SG 40 Particle Size Distribution for DOP

| | |
|---|---|
| 99% | smaller than 3.0 μm |
| 95% | smaller than 1.5 μm |
| 92% | smaller than 1.0 μm |
| 50% | smaller than 0.72 μm |
| 25% | smaller than 0.5 μm |
| 11% | smaller than 0.35 μm |

reported by Virtis, using dioctylphthalate (DOP). The size distribution should be very similar for aqueous solutions. In this study, the size distribution entering the SBS was smaller because the water present in the droplets was evaporated, leaving behind a smaller solid aerosol. The resulting aerosol stream was injected into the main air flow stream.

## 3.4 ANALYTICAL PARTICLE-SIZING EQUIPMENT

A classical scattering aerosol spectrometer (CSAS) manufactured by Particle Measuring Systems was used to determine the concentration and size distribution of the aerosols present in the off gas. On-line sample ports were located at the inlet and outlet of the SBS. Throttling valves were used to maintain a constant flow rate of 17 $m^3/h$ through the instrument. The inlet line to the CSAS was heated to evaporate any entrained water droplets in the off gas and prevent water from condensing on the windows in the sample tube.

The CSAS utilized a He-Ne laser, directed perpendicularly to the gas flow. The beam passed through windows on either side of the pipe in which the gas to be sampled was flowing. Particles present in the off gas caused a pulse of radiant energy during transit through the laser beam. Once it passed through the sample tube, the scattered light was focused onto a detector. The energy of this light was proportional to the size of the particle which caused it to be scattered. The resulting pulse of energy caused a count to be registered in one of 15 channels. Each channel corresponded to a certain energy or size range. A sample could be collected for a given time interval. The number of counts in any channel represented the number of particles in that size range that passed through the laser beam during that period. Calibrating the CSAS

with latex spheres of known size determined the size range corresponding to each channel. The aerosol concentration can be calculated from the number of counts recorded during the sampling period if the flow rate of the sample off-gas stream is known.

# 4.0 EXPERIMENTAL DESIGN

Experiments were usually performed in groups of three to four. The CSAS calibration was verified at either the beginning or the end of each group. Experiments lasted from 20 minutes to 4 hours, depending on the magnitudes of the changes from the previous steady state and the difficulties encountered establishing steady state.

## 4.1 OFF-GAS MAKEUP

For these experiments, the aerosol generator was filled with approximately 40 g of the compound to be resuspended and 3 L of purified water. A sodium chloride solution was used to produce soluble aerosols, while a titanium dioxide suspension was used to generate insoluble aerosols. The air flow rate was set at the desired value by manual adjustment of the DOV. Once a stable air flow rate had been achieved, one of the six Laskin-type nozzles in the aerosol generator was opened. A continuous sample of the inlet off gas was analyzed to determine the aerosol concentration. More nozzles were opened as necessary to increase the concentration. The back pressure to the nozzles was varied to make final adjustments in the aerosol concentration.

The inlet sample port was closed once the off-gas concentration had been set. Steam injection was started at this time if called for by the experimental matrix. The steam injection rate was controlled with a throttling valve. Steam was also introduced to the heat exchanger to bring the inlet temperature to the desired value. The inlet temperature was varied by controlling the steam flow rate to the heat exchanger.

## 4.2 SBS OPERATION

An overflow line maintained the water level approximately 0.3 m above the top of the packing. Makeup water was added as necessary during operating conditions, which caused the off gas to strip water from the reservoir. Manual adjustment of the water flow rate to the two cooling coils maintained the scrubbing water temperature at 20°C. Rotameters indicated the water flow rate through the coils. The SBS was considered to be at steady state when all flow

rates were stable, the inlet off-gas temperature was changing less than 0.1°C/min and the scrubbing solution temperature less than 0.01°C/min.

## 4.3 OFF-GAS SAMPLING

A continuous stream of 17 std $m^3/h$ was taken from the outlet off-gas flow for on-line analysis of the exit particle size distribution. The flow rate through the sample line was determined by using an orifice plate and flanges combined with a differential pressure transducer. The flow rate was controlled by a manual throttling valve. The gas was heated to approximately 80°C prior to entering the CSAS. Once the steady-state exit concentration had been established, the exit sample port was closed and the SBS inlet sampling port opened. Steam injection had to be stopped prior to opening the inlet sample port to prevent steam from condensing on the windows in the sample tube.

Distorted size distributions can be obtained under certain circumstances if isokinetic samples are not taken. Isokinetic sampling requires that the sample tube be oriented directly into the off-gas stream and that the velocity in the sample tube be the same as that of the off-gas stream. The CSAS required a mean sample velocity of 9.84 m/s through the detector. Meeting this constraint as well as the requirements for isokinetic sampling would require a different size sample port for each off-gas flow rate investigated. This procedure was deemed unnecessary for the size distribution being investigated, on the basis of correlations available in the literature (Durham and Lundgren 1980). Samples were taken through 2.5-cm ports which were perpendicular to the off-gas flow. It was also deemed unnecessary to remove any charge the particles received during atomization to prevent sampling losses to the tube walls. This decision was based on criteria presented by Lieu et al. (1985).

## 4.4 CSAS CALIBRATION

The CSAS was calibrated by placing latex spheres of known size in the aerosol generator. The receiving optics were adjusted until the peak produced by the monodispersed aerosol was maximized in the highest possible channel. Three

different sizes of latex spheres were used (0.460, 0.620 and 0.945 μm). A linear relationship between particle size and channel number was assumed between calibration points.

## 4.5 EXPERIMENTAL MATRIX

A partial factorial matrix was completed to test for statistically significant interactions between variables under investigation. Selection of test parameters was based on past experience and information in the literature. Only six parameters were varied in the partial factorial matrix and are listed in Table 3. Three levels of the off-gas flow rate and steam-to-air ratio were investigated. The other four parameters were limited to two levels. Several assumptions were required to reduce the number of experiments to a reasonable number. An iterative program employing a minimized prediction variance criterion was used to construct an experimental design. The resulting partial factorial experimental design consisted of 28 experiments, including three replicates. A full factorial design would have required 144 experiments.

TABLE 3. Values for Experimental Parameters

| Parameters | Levels | | |
|---|---|---|---|
| Superficial Gas Flow Rate (m/s) | 0.48 | 0.34 | 0.21 |
| Steam/Air (std $m^3$/h / std $m^3$/h) | 0.0 | 0.33 | 0.50 |
| Inlet Off-Gas Temperature (°C) | 60 | 100 | |
| Bed Diameter (m) | 0.5 | 0.4 | |
| Packing Size (cm) | 0.3 | 1.0 | |
| Aerosol Species | NaCl | $TiO_2$ | |
| Concentration (particles/cc) | 1000 | | |
| Size Distribution (μm) | 0.3 - 0.7 | | |
| Packing Depth (inches) | 0.55 | | |
| Scrubbing Solution Temperature (°C) | 20 | | |
| Scrubbing Solution Concentration (g captured aerosol/cc) | 0 | | |

## 5.0 INFLUENCE OF VARIOUS PARAMETERS ON THE AEROSOL CAPTURE PERFORMANCE

Completion of the partial factorial matrix described in Section 4.5 showed that all parameters tested were significant. Reducing the full factorial matrix to the 28-test partial factorial matrix had required several assumptions about interactions between parameters. Some of the assumptions were invalid, which resulted in confounding. New assumptions were made before returning to the experimental design program to determine what additional experiments were needed to unconfound the data. Several complete two-parameter factorial experiments were also conducted to illustrate the influence of some of the parameters over specific ranges. In total, 112 experiments were conducted. Summaries of the experiments can be found in Appendix A. The results from the partial factorial matrix will assist in determining the statistical significance of the two-parameter experiments shown later.

In the experiments involving NaCl, it was found that re-entrainment losses predominated over penetration losses, as will be discussed later. As a result, all of the experiments involving sodium chloride aerosols were dropped from the statistical analysis, leaving a total of 69 experiments conducted with titanium dioxide. A linear regression on the data identified seven experiments which were influential in determining the model. These experiments were found to be very different than the other 62 experiments and will be treated separately. Performing a linear regression on the remaining 62 titanium dioxide experiments resulted in the following model:

$$\log(DF) = \beta_0 + \beta_1 F + \beta_2 \alpha + \beta_3 D + \beta_4 P + \beta_5 C + \beta_6 F \cdot \alpha + \beta_7 \alpha \cdot D \qquad (5)$$

where DF = decontamination factor, dimensionless

F = superficial velocity, m/s

$\alpha$ = volumetric steam-to-air ratio, dimensionless

D = bed diameter, m

P = packing diameter, cm

C = inlet aerosol concentration, particles/cc

$\beta_i$ = coefficient

The coefficients for each term can be found in Table 4. This model fits the data very well, accounting for 84% of the variation in the data. The F-test probability that all the coefficients in Equation 5 are equal to zero is less than 0.0001 ($p<0.0001$). All of the main effects investigated, except the inlet temperature, were determined to be significant. Two interaction terms, $F \cdot \alpha$ and $\alpha \cdot D$, were also found to be highly significant. The log of the DF is used to transform the data so that the residual errors follow a normal distribution (Ostle and Mensing 1982).

## 5.1 SIMULATION OF IMPORTANT COMPOUNDS IN LFCM OFF GAS

Radioactive cesium and ruthenium aerosols are the key particulates that must be removed from LFCM off gas (Kitamura et al. 1986). Therefore, it is desirable to choose the primary scrubber on the basis of its ability to remove these compounds. Cesium usually leaves the melter in the form of oxides, chlorides and/or nitrates, depending on the composition of the feed. These compounds should behave like their sodium analogs, since sodium and cesium are in the same group of the periodic table. The wettability of an aerosol is probably the most important characteristic, next to particle diameter, in determining the efficiency at which it will be removed from the off gas. For this reason it was felt that sodium chloride could be used to represent all of the cesium compounds, since the cesium compounds of interest are all highly soluble in water. Ruthenium aerosols are usually found as oxides which are insoluble

TABLE 4. Parameter Estimates

| Coefficient | Coefficient Estimate | Standard Error | Probability of Coefficient=0 |
|---|---|---|---|
| $\beta_0$ | 1.53 | 0.146 | 0.0001 |
| $\beta_1$ | -0.734 | 0.0920 | 0.0001 |
| $\beta_2$ | -1.12 | 0.477 | 0.0222 |
| $\beta_3$ | -1.93 | 0.200 | 0.0001 |
| $\beta_4$ | 0.120 | 0.0290 | 0.0001 |
| $\beta_5$ | 0.000196 | 0.0000918 | 0.0369 |
| $\beta_6$ | -1.80 | 0.465 | 0.0003 |
| $\beta_7$ | 3.96 | 1.08 | 0.0006 |

in water. Titanium dioxide was used to simulate ruthenium dioxide, since both are insoluble in water and are relatively close together in the periodic table. Simulants for cesium and ruthenium were used to reduce the cost of the experiments.

One experiment was repeated several times under the same experimental conditions but with different compounds in the aerosol generator. This experiment was used to demonstrate the ability of sodium chloride and titanium dioxide to simulate cesium and ruthenium compounds, respectively. A 0.5-m bed filled with 0.36 m of 0.3-cm packing was used. The off-gas flow rate was maintained at 127 std $m^3/h$. Once the inlet concentration was set at 1000 particles/cc, the on-line analysis was switched to the outlet sample port. An outlet particle distribution was measured when steady state had been achieved. The aerosol generator was then shut off, and a new outlet particle distribution was measured. The second measurement provided information as to how many of the aerosols coming out of the SBS actually penetrated the SBS and how many were entrained from the scrubbing solution by the vigorous agitation induced by bubbles bursting at the surface of the aqueous pool in the SBS.

Several important conclusions can be drawn from the results, which are shown in Table 5. First, it appears that the outlet aerosol concentration is the same regardless of whether or not the aerosol generator is on when comparing the results of the three soluble compounds (NaCl, CsCl and $CsNO_3$). This result suggests that there are no soluble aerosols penetrating the SBS and that the particles in the outlet stream are being re-entrained from the scrubbing solution. These results imply that sodium can be used to simulate cesium,

TABLE 5. Influence of Aerosol on SBS Performance

| Run Number | Aerosol | Grams/3.0 L Purified Water | Inlet Conc. Particles/cc | Outlet Conc. Particles/cc | Re-Entrained[a] Particles/cc | Mass DF |
|---|---|---|---|---|---|---|
| 108 | NaCl | 30 | 1097 | 38 | 48 | 26.7 |
| 109 | CsCl | 50 | 1056 | 45 | 52 | 20.0 |
| 110 | $CsNO_3$ | 57 | 1092 | 56 | 55 | 18.4 |
| 111 | $TiO_2$ | 50 | 1088 | 167 | 54 | 5.6 |
| 112 | $RuO_2$ | 100 | 787 | 207 | 54 | 3.9 |

(a) Measured outlet concentration with aerosol generator off.

although there are not many meaningful tests that can be performed with sodium chloride because the capture efficiency is limited by re-entrainment. This theory implies that there exists an upper limit on the obtainable mass DF that is controlled by the amount of material being re-entrained. The mass DF is defined as the ratio of the aerosol mass flow rate in divided by the aerosol mass flow rate out, Equation 6:

$$\text{mass DF} = \frac{m_{(in)}}{m_{(out)}} \tag{6}$$

where

$$m_{(out)} = m_{(penetration)} + m_{(re\text{-}entrainment)} \tag{7}$$

Aerosols in the outlet stream can follow one of two paths through the SBS. Aerosols can remain in the off gas as it passes through the SBS, in which case they would be included in $m_{(penetration)}$, the mass flow rate out due to penetration. An aerosol can also be re-entrained after being captured. As the bubbles break through the surface of the aqueous pool, small droplets of scrubbing solution are sheared off and carried away by the off gas. As the scrubbing solution evaporates, any residual material will be left behind in the form of an aerosol. These particulates are included in the mass flow rate out due to re-entrainment, $m_{(re\text{-}entrainment)}$. For the experiments conducted with soluble aerosols, the re-entrainment term dominates the penetration term, making it impossible to determine anything about the influence of various parameters on the removal of soluble particles. The captured aerosol concentration in these experiments was actually insignificant, but the optical sizing equipment could not distinguish between a sodium chloride aerosol and a silica aerosol. The SBS was filled with fresh process water, but the impurities present in the water and the resuspension of residual material in the SBS, as well as attrition of the packing, resulted in a high enough concentration of material in the scrubbing solution to produce submicron aerosols. This phenomenon suggests that efforts to improve efficiency should be directed toward reducing re-entrainment, as opposed to improving the initial capture of these soluble compounds.

The insoluble aerosols did not show the same trend. The outlet concentration during the experiment was much higher than the re-entrainment concentration measured after the experiment for both titanium and ruthenium dioxides. This result implies that there is significant penetration of insoluble aerosols through the SBS. There was not enough ruthenium dioxide available to achieve the concentration in the aerosol generator necessary to produce an inlet concentration of 1000 particles/cc. It is still apparent that ruthenium behaves reasonably like titanium, and was therefore replaced by titanium dioxide in all experiments. Even though re-entrainment contributes significantly to the exit mass flow rate, the penetration term dominates the total exit mass flow rate to the extent that the influence of various parameters on scrubbing performance can be accurately measured for insoluble aerosols.

## 5.2 INLET AEROSOL CONCENTRATION

The previously described experiment suggested that all of the incoming soluble aerosols were being captured, so a second experiment involving sodium chloride aerosols was conducted to further investigate this result. A 0.4-m-diameter bed was filled to a depth of 0.5 m with 1-cm ceramic spheres. The off-gas flow rate was maintained at 51 std $m^3/h$ and an inlet temperature of 100°C. The scrubbing solution was maintained at 20°C. The inlet aerosol concentration was then varied from 500 particles/cc to 27,000 particles/cc. Figure 5 shows that the scrubbing performance increases with increasing inlet concentration. This is a characteristic not common to all air filtering devices. Also shown is the outlet concentration versus inlet concentration. The outlet concentration appears to be independent of the inlet concentration, having an average value of approximately 30 particles/cc. This result confirms the hypothesis that scrubbing performance of soluble aerosols is re-entrainment limited. Concentration limitations on the particle-sizing equipment prevented higher inlet concentrations from being investigated. It appears that the SBS can handle larger inlet concentrations of soluble aerosols without significant penetration resulting.

A similar experiment was not conducted for titanium dioxide, but the linear regression performed on the titanium dioxide experiments showed that the

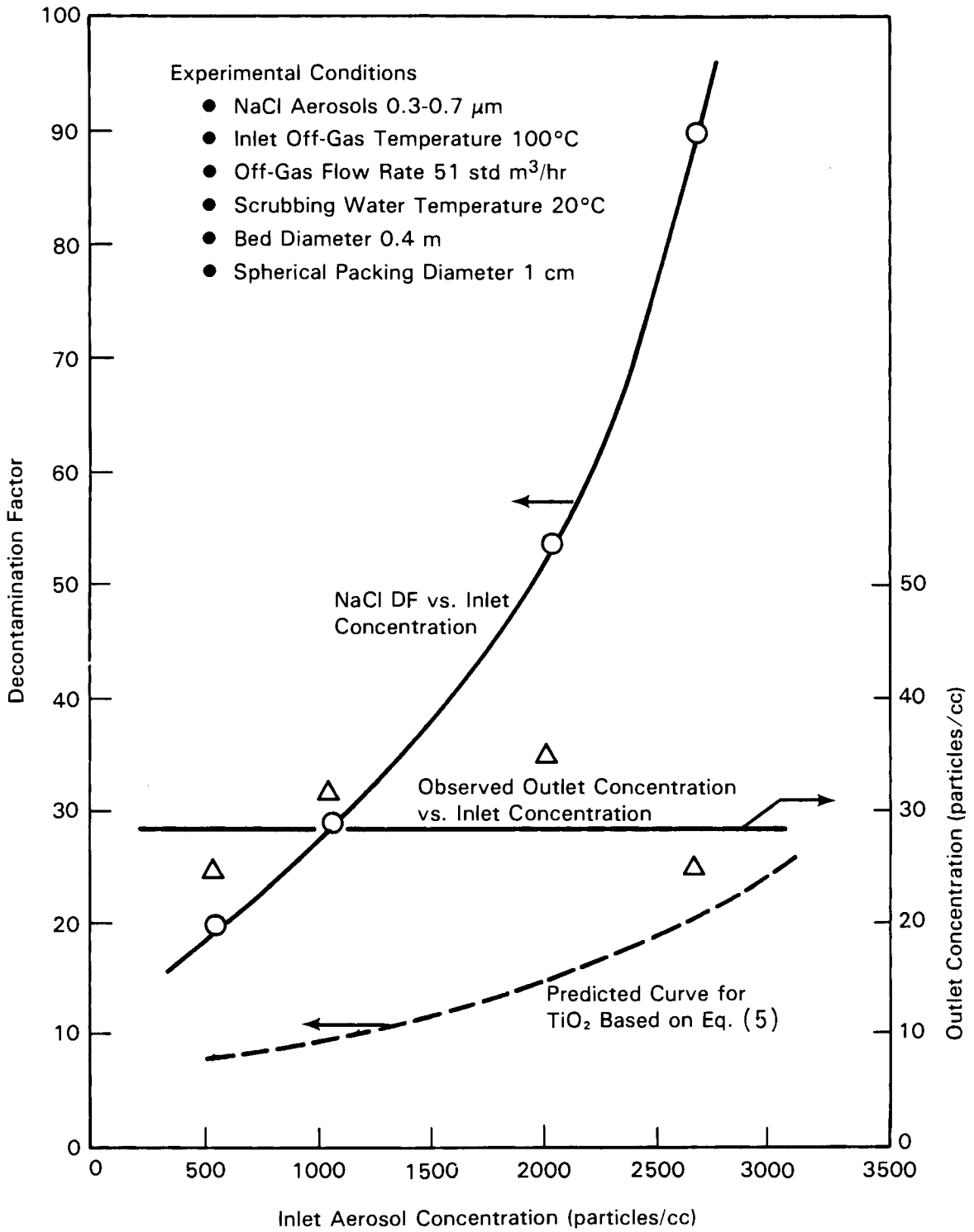


FIGURE 5. Influence of Inlet Concentration on SBS Performance

coefficient for the concentration term in the model was highly significant ($p = 0.04$). The scrubbing performance also increased with inlet concentration for insoluble aerosols, yet the effect was not nearly as pronounced. The predicted influence of inlet concentration on performance is shown in Figure 5 for titanium dioxide aerosols based on Equation 5. The effect of concentration on scrubbing performance may be more significant at higher values where coagulation due to Brownian motion will be more important. The inlet concentration for titanium dioxide ranged from 800 to 1300 particles/cc, which was much smaller than the corresponding range investigated for sodium chloride. The model is extrapolating out to a region where there are no data to complete the titanium dioxide curve shown in Figure 5. Therefore, this curve should be used with caution.

## 5.3 HUMIDITY

As previously mentioned, the primary concern of the SBS to the nuclear waste processing industry is its ability to remove aerosols containing cesium and ruthenium. These compounds are semivolatile at the conditions present in the melter. As the off gas cools upon leaving the melter, the cesium and ruthenium compounds condense, forming submicron aerosols (Scott, Goles and Peters 1985). The resulting aerosols fall into the "most difficult to capture" size range (Hinds 1982; Shaw 1978). One approach to increasing the capture performance would be to shift the size range of these particles. As mentioned in Section 2.3, this objective can be achieved by adding steam to the off gas. As the off gas is cooled, the water vapor will begin to condense on nucleids before undergoing homogeneous nucleation; thus, the steam should tend to condense on the aerosols present in the off gas, causing the particles to grow in size and making them easier to capture. This process may also improve the ability of insoluble aerosols to be captured, because they will become "prewetted." Several experiments were conducted using titanium dioxide aerosols to test this theory. A 0.5-m-diameter bed filled with 0.55 m of 1-cm ceramic spheres was used in the SBS. The gas contained 1000 particles/cc of titanium dioxide aerosols in the 0.3-μm to 0.7-μm size range and was maintained at an inlet temperature of 100°C. Again, the scrubbing solution was held at 20°C.

The volumetric steam-to-air ratio was varied from 0 to 0.5 while the superficial air velocity ranged from 0.14 to 0.48 m/s.

Figure 6 shows the family of curves relating the influence of the steam-to-air ratio on SBS performance as a function of the superficial air velocity. Relatively smooth curves were generated for all three steam-to-air ratios investigated. There was a significant increase in the scrubbing performance when steam was first added to the off gas. Increasing the ratio from 0.33 to 0.5 showed a modest increase in performance. These results are consistent with the theory presented in Section 2.3. It can also be seen that the scrubbing performance decreases as the superficial velocity increases. This result is consistent with the aerosol capture mechanisms presented in Section 2.2. Aerosols in the submicron size range should be captured predominantly by

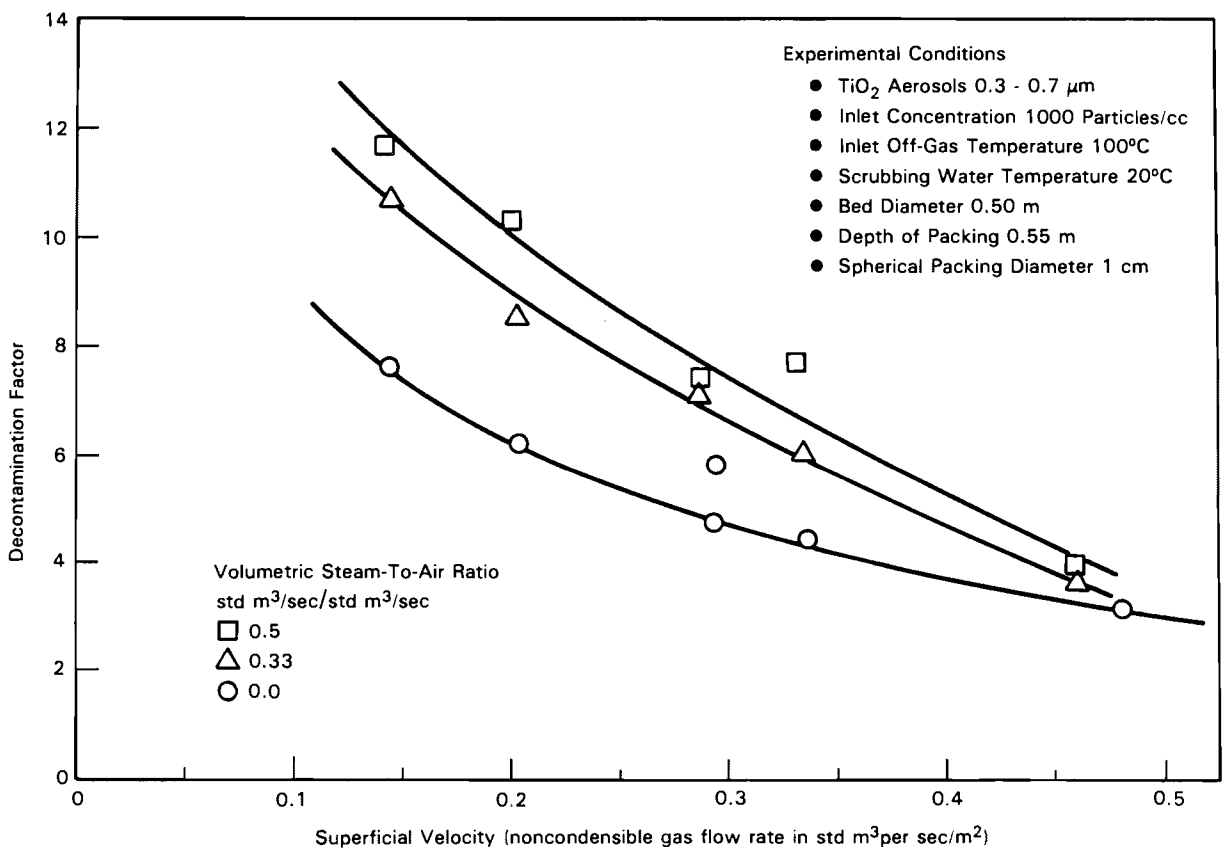


FIGURE 6. Influence of Steam on SBS Performance ($TiO_2$)

interception and Brownian motion. The former capture mechanism is independent of flow rate, while the latter results in higher capture efficiencies at lower flow rates.

Re-entrainment is another parameter influencing the shape of these curves that was not considered. As seen in Table 5, the re-entrained aerosol concentration can be a significant portion of the aerosol concentration leaving the SBS. The degree of re-entrainment depends on the superficial air velocity; the higher the velocity, the more material will be re-entrained. The decrease in the mass DF at higher velocities is probably due more to increases in the re-entrainment term in Equation 7 than to increases in the penetration term. This phenomenon tends to lower the right-hand portion of the curves in Figure 6. At the highest velocity, in fact, the presence of steam appears to have little influence on the scrubbing performance. It is possible that the residence time is reduced sufficiently, at this velocity, that full advantage cannot be taken of the condensing steam. It is more likely, however, that re-entrainment is so high that any improvements in the $m_{(penetration)}$ term, in Equation 7, that are due to steam are completely hidden by the dominance of the term due to re-entrainment.

The same set of experiments was repeated using sodium chloride aerosols. The results are shown in Figure 7. In this case, no consistent trend relating scrubbing performance to superficial velocity can be found. The random pattern is observed because the DF is limited by re-entrainment for soluble aerosols. The varied data reflect the sporadic nature of the re-entrainment mechanism. The inlet mass flow rate is very high compared to the outlet mass flow rate, so small changes in the re-entrainment concentration result in large changes in the inlet/outlet ratio. Although no trend can be found in the data, the experiments do show that the mass DF for the soluble sodium chloride is generally an order of magnitude higher than the corresponding DFs for insoluble titanium dioxide aerosols. These results, combined with the earlier results for soluble aerosols, suggest a greatly increased potential for using the SBS to capture soluble aerosols if the SBS can be modified and/or operated such that re-entrainment from the scrubbing solution can be eliminated.

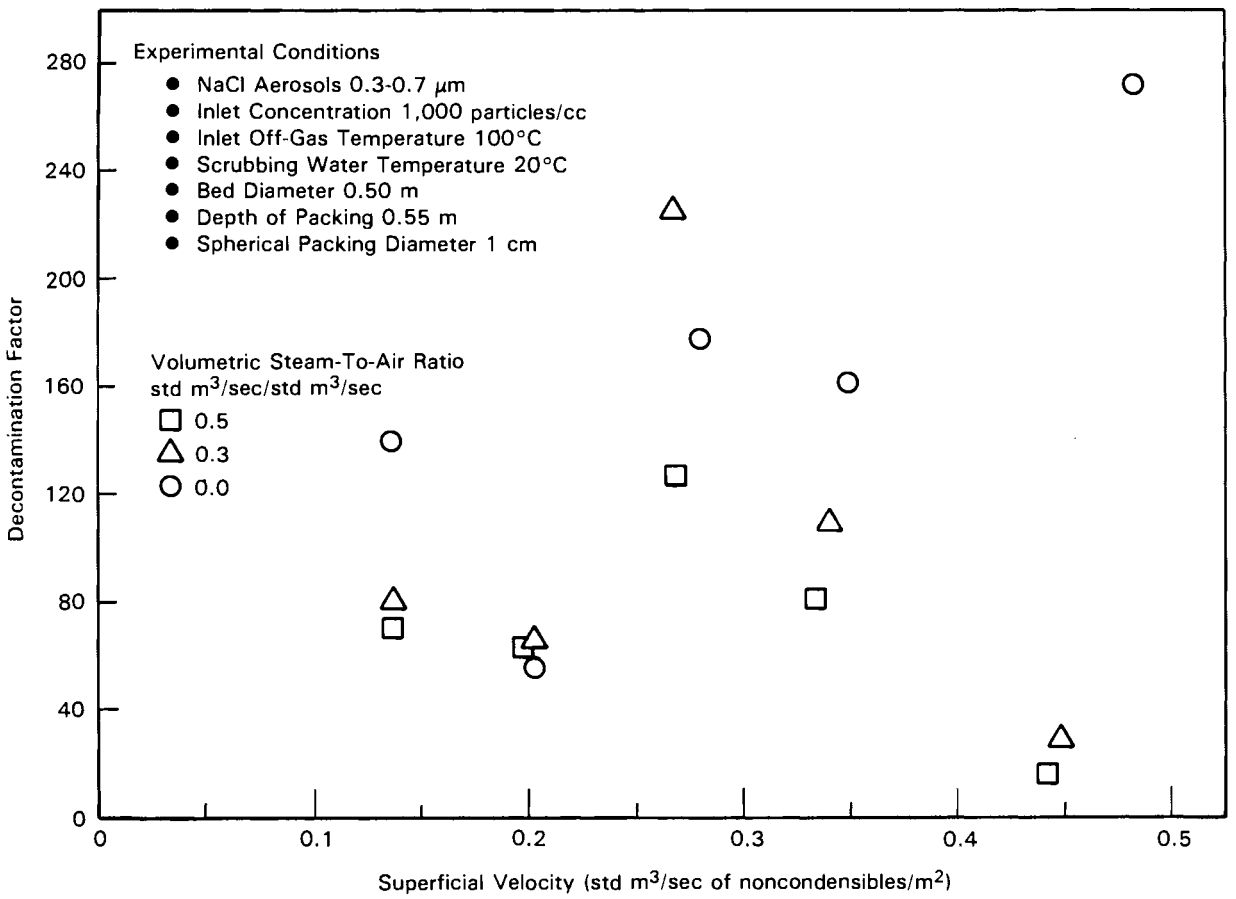


FIGURE 7. Influence of Steam on SBS Performance (NaCl)

## 5.4 BED DIAMETER

No special attempt was made to ensure that the off gas was being evenly distributed across the inlet of the packing. Visual observation through 0.1-m view ports in the lid of the SBS (located directly above the packing) showed that the frothing was more vigorous next to the gas inlet pipe. It was difficult to quantify the nonuniformity of the gas distribution as the bed was not visible below the liquid level. To vary the bed diameter, a sleeve was designed to fit inside the original 0.5-m-diameter bed, reducing the diameter to 0.4 m. This sleeve changed the cross-sectional area from 0.172 $m^2$ to 0.099 $m^2$. The cross-sectional areas have been corrected for the area occupied by the downcomer assembly (0.17 m O.D.). Experiments were then conducted in

which four different bed configurations were compared at various superficial air velocities. Both bed diameters were investigated using 1-cm and 0.3-cm ceramic packing.

If the gas is distributed evenly across the packing for two different bed diameters containing the same packing, the performance should be the same as long as the volumetric flow rates are adjusted such that the velocities through the beds are equal. This result can be achieved by setting the ratio of the volumetric flow rate to the cross-sectional area equally for the two beds. Any difference in performance between equivalent experiments can be attributed to inlet distribution problems.

The results shown in Figure 8 suggest that both packing size and bed diameter influence the scrubbing performance. The small-diameter bed outperformed the larger bed regardless of which packing was used. This observation is

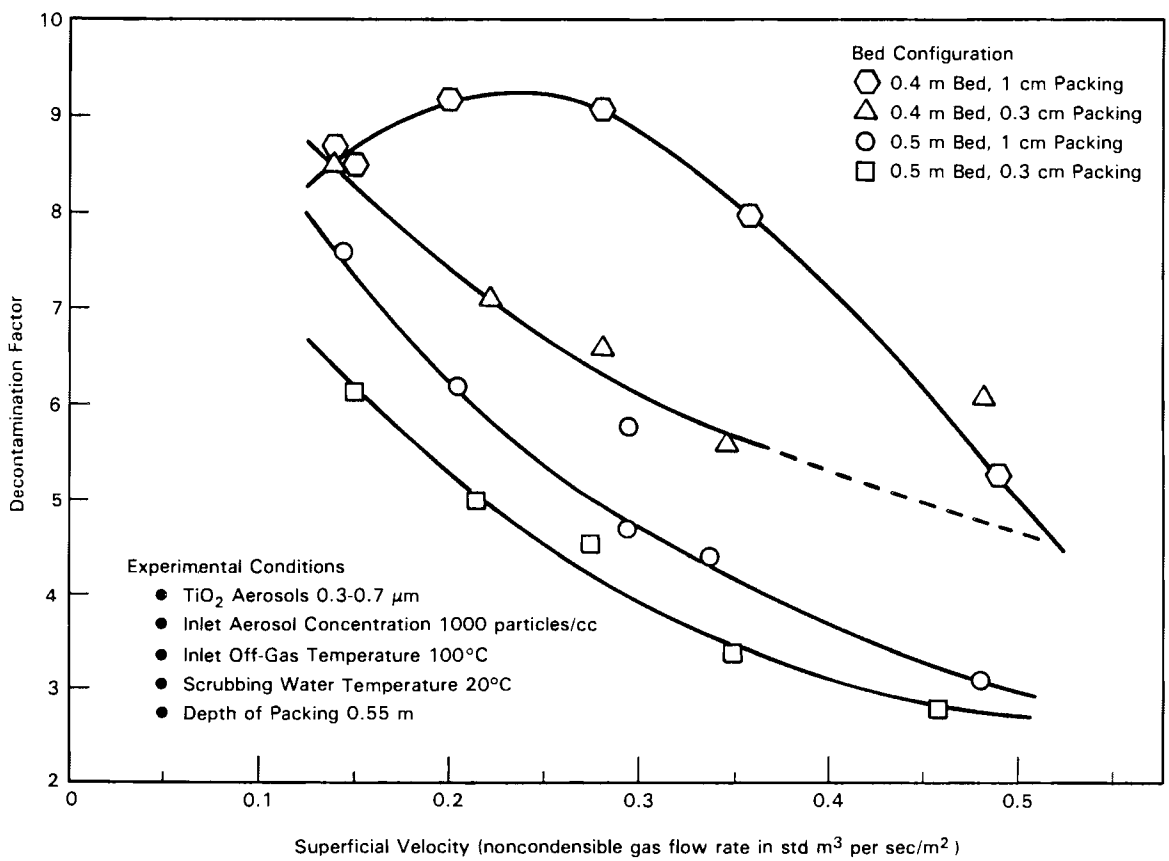


FIGURE 8. Influence of Bed Diameter on SBS Performance

confirmed by the results of the linear regression. The main effect due to the bed diameter was found to be highly significant ($p = 0.02$), as well as an interaction term involving bed diameter and the steam-to-air ratio ($p = 0.006$), where the Student's t-test p valve is the probability that the coefficient of interest is not significantly different than zero. These results indicate a gas distribution problem. If the gas distribution is poor, the actual flow rate through the bed will be higher than expected. The higher flow rate lowers the mass DF by increasing both the exit mass flow rate due to penetration and re-entrainment. The penetration term increases because there is less time for the aerosols to migrate to the collecting medium through Brownian motion. The re-entrainment term increases because of the extra kinetic energy associated with the higher flow rate. Gas distribution problems probably exist with the small-diameter bed as well, at low flow rates. This explanation may account for the sudden decrease in performance at low velocities for the 0.4-m bed containing 1-cm packing. Under these conditions, the gas is probably channeling up through the packing close to the inlet pipe, where the void fraction is highest.

Figure 8 includes only conditions that do not involve steam. The model derived from a linear regression of the data shows that there is a significant two-way interaction between the bed diameter and steam-to-air ratio. Figure 9 shows the predicted interaction between the bed diameter and steam-to-air ratio for a given set of experimental conditions. The small bed should have a better gas distribution at equal superficial velocities, because the gas does not have to travel as far radially before it starts up the bed. A more uniform distribution should lead to larger DFs, since it will result in lower bed velocities, which enhances the aerosol capture mechanism due to Brownian motion. At a superficial velocity of 0.30 m/s and a steam-to-air ratio of zero, the predicted performance decreases as the bed diameter increases. This result can be easily explained by the preceding argument if one accepts the assumption that the gas distribution is better in the smaller bed; the gas does not have as far to travel radially before starting up through the bed, and lower bed velocities result. As steam is added, the total volumetric flow rate increases while the superficial velocity of noncondensible gases remains the same. The steam will increase the size of the gas bubble under the packing,

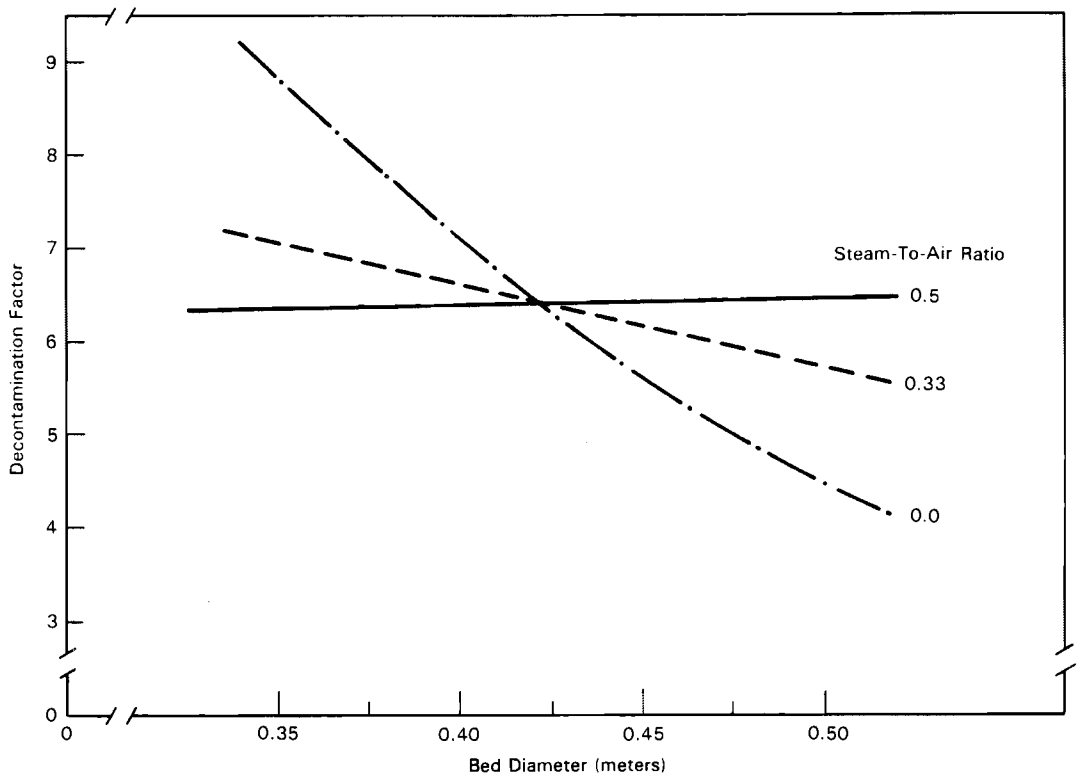


FIGURE 9. Predicted Interaction Between Bed Diameter and Steam-to-Air Ratio at a Superficial Velocity of 0.3 m/s

resulting in better gas distribution as well as larger DFs. As the gas distribution becomes more complete, the performance of the two beds should become equal. The predicted DFs do in fact become equal, as evidenced by the horizontal line, once the steam-to-air ratio reaches 0.5.

## 5.5 PACKING SIZE

Air-cleaning devices generally exhibit a minimum collection efficiency at a given aerosol diameter. This minimum is typically in the 0.1 to 1.0-micron range. Figure 10 shows that it occurs at approximately 0.5 micron for the SBS. The interception capture mechanism plays a major role in aerosol removal in this region of minimum efficiency. The collection efficiency by interception can be improved by increasing the ratio of the aerosol particle diameter to the packing diameter (Hinds 1982). Therefore, according to theory, the 0.3-cm

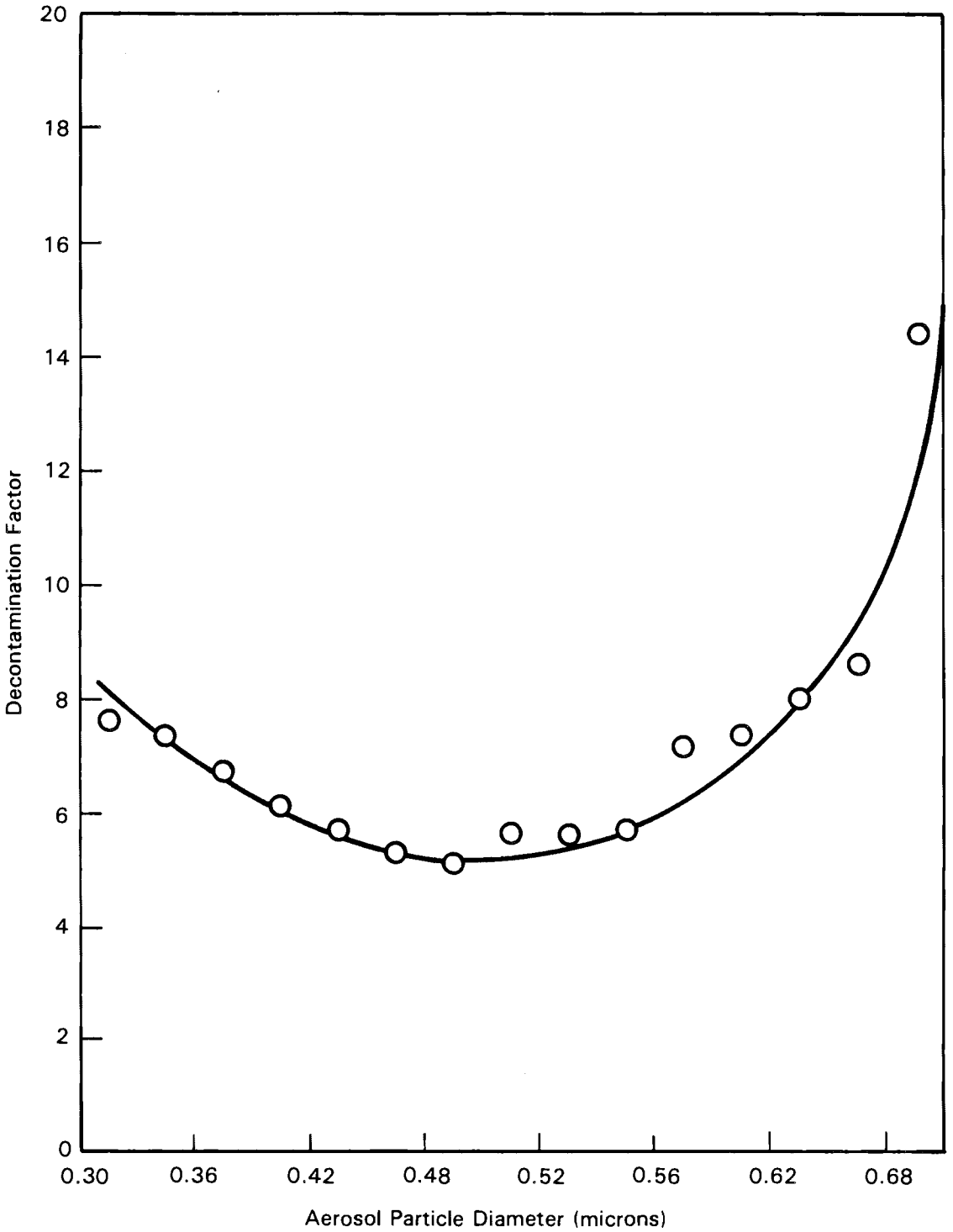


FIGURE 10. Collection Efficiency as a Function of Particle Diameter

packing should work better than the 1-cm packing. As seen in Figure 8, this is not the case. For a given bed diameter, the 1-cm packing resulted in a larger DF.

A small-scale plexiglass model of the SBS was constructed in an attempt to detect any significant differences in the flow pattern through the two different packing sizes. As expected, the smaller packing led to better inlet gas distribution, but the flow patterns through the two beds were quite different. Bubbles remained discrete in the large packing, while channels containing a continuous gas phase formed in the small packing. The residence time in the bed was probably much shorter in the small packing than for the rising bubbles observed in the 1-cm packing, and this shorter residence time could explain the decrease in performance. Although the interception capture mechanism may improve with smaller packing, it is not the only capture mechanism at work. Removal by Brownian diffusion is very important for the aerosol size range investigated. The Brownian motion capture mechanism will become more effective at longer residence times. Thus, any increase in performance resulting from capture by interception in the bed containing small packing was more than offset by the decrease in the effectiveness of the Brownian motion capture mechanism.

## 5.6 INLET TEMPERATURE

It was expected that the inlet temperature of the off gas should have an effect on scrubber performance, since many of the aerosol transport mechanisms discussed in Section 2.1 are temperature dependent. The maximum inlet temperature was limited to 100°C because of limitations on the building steam supply and the size of the heat exchanger used. A lower temperature of 60°C was chosen, as temperatures below 60°C were unachievable at steam-to-air ratios of 0.5 without cooling of the off gas. The operating range of 60° to 100°C was very small and not representative of melter off gas (200° to 400°C) but was included as a parameter in case temperature effects were significant enough to influence scrubbing performance even for small changes in the inlet temperature. Increased temperatures increase aerosol movement. Since some external force is necessary to drive an aerosol from a streamline to a collecting surface, any

increase in movement should result in higher capture efficiencies. If there were no external driving forces, aerosols would only be removed by interception.

Figure 11 shows the results from several experiments repeated for inlet temperatures of 60° and 100°C using a 0.5-m-diameter bed filled with 0.55 m of 0.3-cm ceramic spheres. No detectable influence of inlet temperature on aerosol scrubbing performance is indicated for the range investigated. This result was statistically confirmed by the linear regression. The main effect of inlet temperature on scrubbing performance was not significant, nor were any interactions between the inlet temperature and other parameters. Including the main

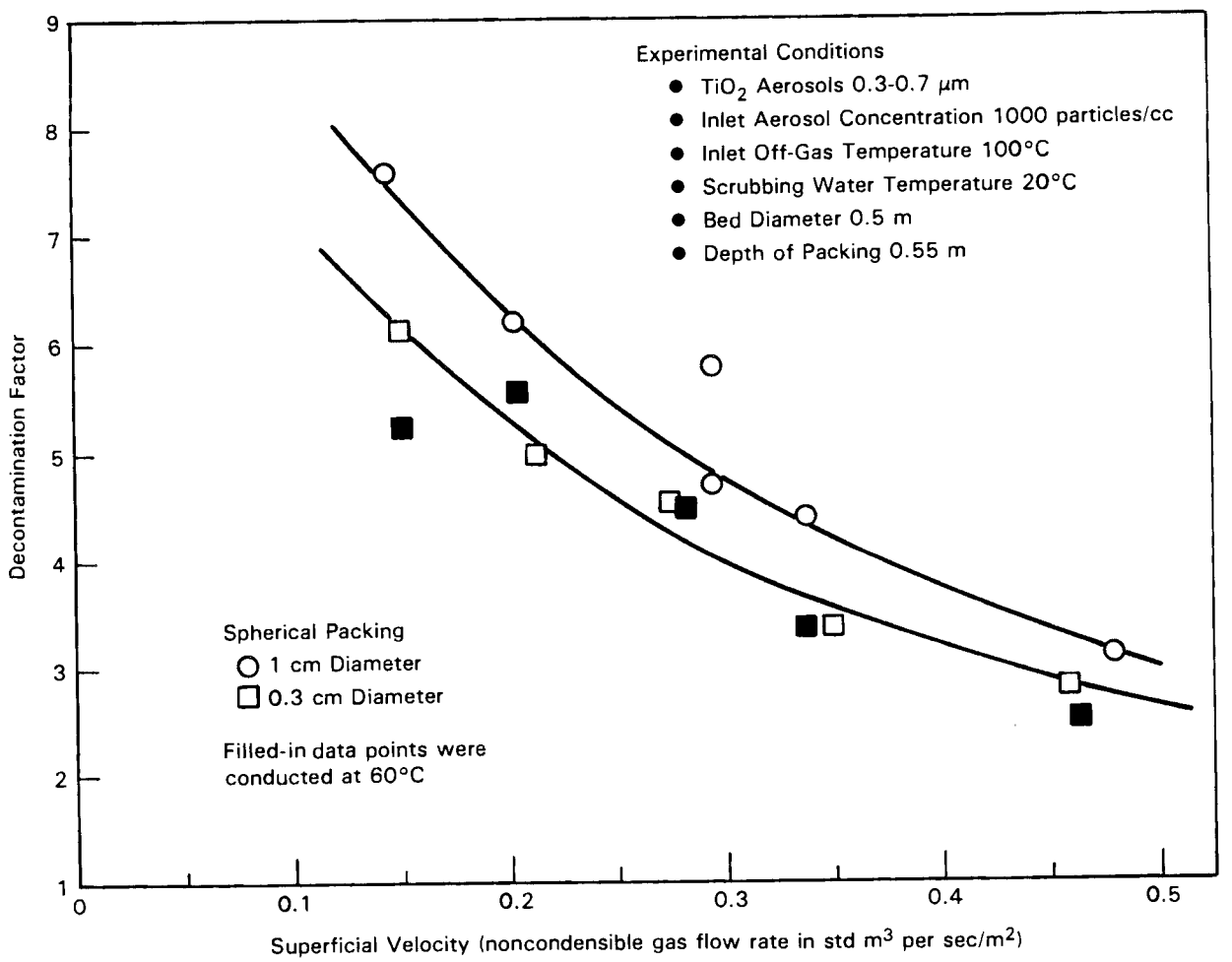


FIGURE 11. Influence of Packing Size on SBS Performance

effect of the inlet temperature in the previous model resulted in a t-test probability of 42%. This test implies that even though the linear regression calculated a value for the inlet temperature coefficient, the probability that the coefficient is not significantly different from zero is 42%. Although the inlet temperature was not determined to be significant, it may be inaccurate to assume that it will not have an effect at higher temperatures. It is important to keep this fact in mind when using the model given in Equation 5 to predict mass DFs outside of the range of experimental values.

The inlet temperature probably has little influence on the scrubbing performance for the range of temperatures investigated as a result of the rapid quenching occurring once the off gas enters the bed. As can be seen in Figure 12, the off-gas cools very quickly as it passes through the bed. The inlet temperature measured at the bottom of the bed in the axial thermowell varied constantly with the pulsing of the off-gas flow rate but was approximately 60°C colder than the inlet temperature measured by a thermocouple located directly in the path of the off gas. There was little difference in the axial temperature profile between inlet temperatures of 60° and 100°C, which is probably one of the reasons that the inlet temperature did not seem to affect the performance.

The axial temperature profile does not, however, represent the only important temperature influencing the aerosol capture performance. While the axial temperature is probably a good indication of the gross movement of the aerosols in the bubble, the radial temperature profile within the bubble is more important in determining the net movement. The slope of the temperature gradient is in part determined by the inlet temperature and the temperature of the scrubbing solution. The gas is hottest at the center of the bubble and cools down to temperatures approaching that of the scrubbing solution at the gas-liquid interface. Aerosol scrubbing efficiencies should be increased, if the inlet conditions can be raised sufficiently to establish a temperature gradient inside the bubble. Thermophoresis increases the particulate movement down the temperature gradient, forcing the aerosols towards the gas-liquid interface.

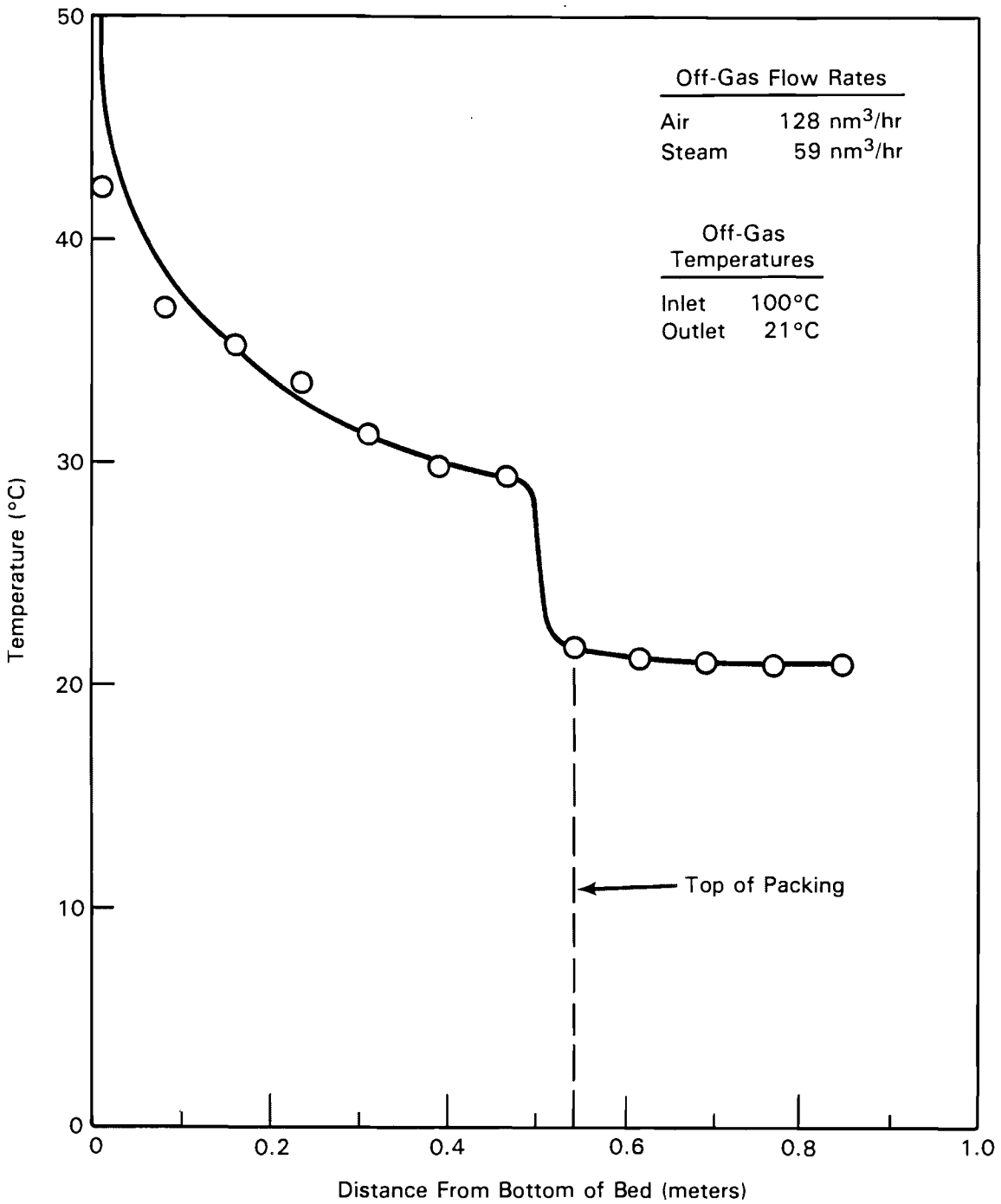


FIGURE 12. Typical Axial Bed Temperature Profile

This effect will probably not become significant until the temperature difference between the center of the bubble and the gas-liquid interface is closer to 400°C than to 80°C.

A higher inlet temperature is desirable, because it would allow greater steam-to-air ratios without the off gas becoming saturated. Several effects would be combined to help capture aerosols in this case:

1) Off gas entering the inlet gas distributor saturated with steam at 400°C would produce bubbles that would diminish in size as the scrubbing solution cooled the off gas. Both an overall reduction in mass as steam condensed and volumetric changes caused by decreases in the gas temperature would contribute to reduction in the size of the bubble. The transport distances to the collecting medium would be shortened, which should result in a higher collection efficiency. A high ratio of steam would be necessary to significantly decrease the transport distances inside a bubble, because the diameter of a bubble is proportional to the cube root of the volume. A large decrease in the bubble volume only produces small changes in the diameter.

2) The aerosol concentration would increase as the volume of the bubble decreased. As the concentration increased, Brownian motion would produce more interactions between aerosols, resulting in agglomerated particles that would be easier to remove.

3) As previously mentioned, steam would start to condense as the off-gas temperature dropped. Most of the condensation would occur at the gas-liquid interface, producing an aerodynamic draft directed towards the interface known as Stephan flow, which is described in Section 2.1. Some steam will condense on aerosols present in the bubble, resulting in larger particles that would be easier to capture. Other effects may be present, such as thermophoresis and diffusiophoresis. These are sometimes referred to collectively as flux-force/condensation (Calvert and Jhaveri 1974).

4) The insoluble aerosols pre-wetted by condensing steam would become pseudo-soluble aerosols that would be more susceptible to being captured.

The combined influence of the above effects could possibly make the inlet temperature an influential parameter at temperatures above those investigated in this study.

## 5.7 EFFECT OF SUB-DEW-POINT INLET CONDITIONS

A linear regression was performed on the original 69 experiments using titanium dioxide. The resulting model contained 17 significant terms, including the main effect due to all parameters investigated as well as four 3-way interactions and several 2-way interactions. An inspection of the model revealed that it was severely influenced by a handful of experiments; the five tests having the highest DFs. The dew points for steam-to-air ratios of 0.33 and 0.5 are approximately 65° and 71°C, respectively. All five of the experiments with high DFs had two characteristics in common: 1) they had steam-to-air ratios of 0.33 or 0.5, and 2) the inlet temperatures were 60°C. The inlet conditions of these experiments were such that the off gas was entering the SBS below its dew-point temperature, so some condensation must have been occurring in the downcomer. A complete list of the sub-dew-point experiments, as well as their predicted DFs using Equation 5 is shown in Table 6.

TABLE 6. Experiments Conducted at Inlet Temperatures Below the Dew Point

| Run # | Superficial Velocity | Inlet Temperature | Steam/Air Ratio | Actual DF | Predicted DF |
|---|---|---|---|---|---|
| 5 | 0.18 (m/s) | 62.9 (°C) | 0.42 | 39.9 | 9.8 |
| 6 | 0.20 | 59.2 | 0.34 | 58.8 | 8.0 |
| 24 | 0.34 | 59.4 | 0.34 | 15.9 | 5.4 |
| 33 | 0.21 | 60.3 | 0.48 | 43.2 | 7.3 |
| 36 | 0.46 | 58.0 | 0.34 | 4.1 | 2.5 |
| 71 | 0.46 | 58.3 | 0.34 | 8.4 | 3.9 |
| 77 | 0.35 | 64.0 | 0.49 | 43.3 | 5.3 |

The DFs for these experiments were much higher than the values predicted by the model. The two low values, runs 36 and 71, were at the upper end of the flow range investigated. The re-entrainment during these experiments would be significant enough to mask most of the effects due to the sub-dew-point inlet conditions.

The overall results of all of the seven runs suggest that the inlet temperature will have little influence on the scrubbing performance until it drops below the dew point of the off gas. Whether the temperature of the gas entering the SBS is above or below the dew point probably determines where the steam will condense. If the off gas is already below the dew point before entering the SBS, some condensation of steam must have occurred. In this situation, the steam will condense on the aerosols, making them larger and "pre-wetted." These developments will improve the capturability of the aerosols. If the inlet temperature is above the dew point, the steam will not condense until the off gas has contacted the scrubbing solution. At this point, the steam will preferentially condense at the gas-liquid interface and not on the aerosols. Although this action results in Stephan flow towards the interface, as mentioned before, it is obviously not as effective as when steam condenses on the aerosols themselves.

If the flow rate is slow enough, and the steam-to-air ratio high enough, it is possible to force steam condensation on the aerosols even when the inlet condition is above the dew point. Run #44 fits this description and happens to have the highest DF (11.7) of any of the experiments conducted at inlet conditions above the dew point. These results point out the importance of controlling when and where the steam condensation occurs when operating an SBS. A significant improvement can be obtained if the off gas contains condensible gases and can be cooled below the dew point before it enters the SBS.

## 5.8 RE-ENTRAINMENT

After prolonged use, the scrubbing solution in the SBS will have a significant concentration of captured material that has the potential of being re-entrained. This problem can be minimized by injecting large volumes of water into the SBS, either in the form of steam in the off gas or as makeup

water. The liquid circulation rate can then be maintained at a level sufficient to prevent the water in the SBS from becoming concentrated with captured aerosols. This procedure results in large volumes of water that must be reprocessed, depending on the nature of the material being captured. The water would have to be treated as low-level waste if the SBS were being used for scrubbing off gas generated during nuclear waste processing. Hence, it would not be desirable to solve the problem by creating large volumes of contaminated water.

An initial concern was how re-entrainment was varying with time, as experiments were generally conducted in groups of three. The amount of material being captured by the SBS during one experiment was so small that it was impossible that this was the material being re-entrained. A likely candidate appeared to be the residual material, such as rust that was present in the SBS, as well as pieces of packing that might break off during an experiment because of agitation in the bed. An experiment was conducted in which the SBS was operated at severe inlet conditions (high inlet temperature and gas flow rate) for 24 hours to determine whether re-entrainment was a function of time. The results of this experiment are plotted in Figure 13. As can be seen, the outlet concentration did not change with time, maintaining a nearly constant value of 19 particles/cc. Those particles coming out of the SBS represent re-entrained particles since the aerosol generator was not used, so the only aerosols entering the SBS would be those already present in the room air. The data do not indicate any effect, over time, from re-entrainment, so experiments can be conducted in groups without confounding the data.

The origins of the particles composing the outlet concentration shown in Figure 13 are not known for certain. The particles detected by the CSAS leaving the SBS probably come from re-entrained material present in the scrubbing solution, water droplets that do not completely evaporate before entering the CSAS (operated at inlet temperatures around 80°C), aerosols present in the room air that penetrate the SBS and/or material flaking off of the walls of the carbon steel sample lines. Inductively coupled plasma (ICP) analysis of the scrubbing water after a typical experiment indicated that the individual concentration of any one element was not very high. The total concentration of

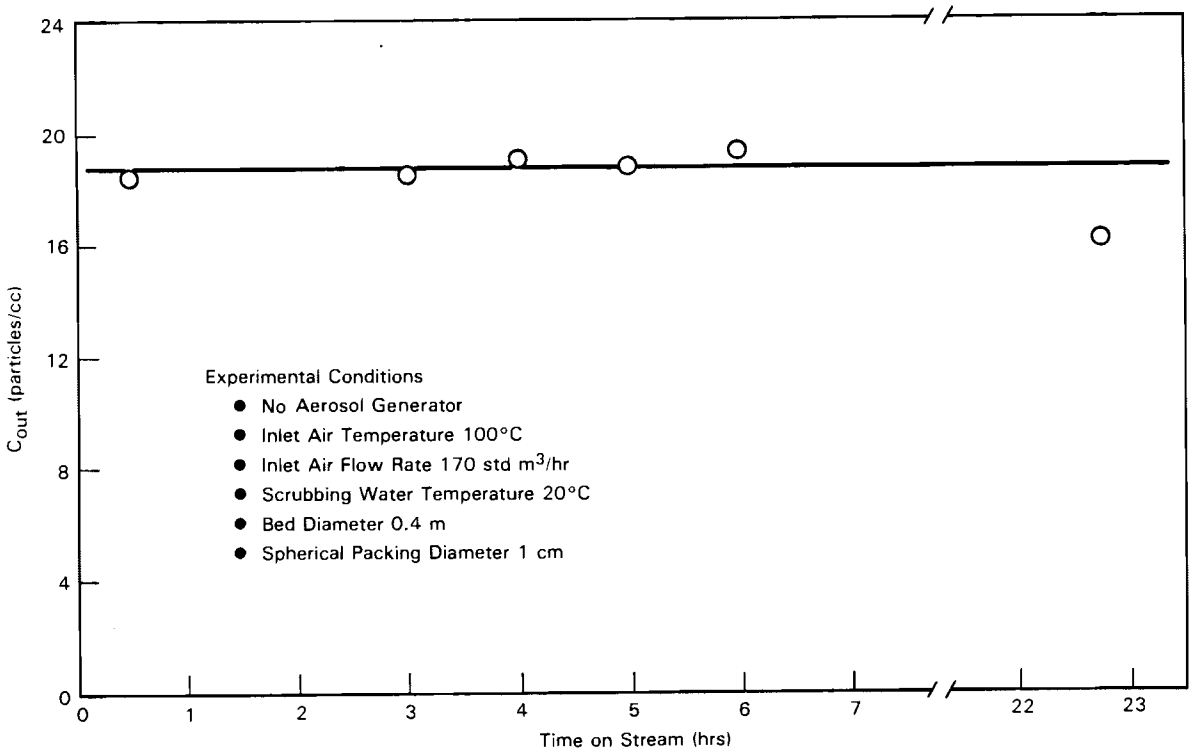


FIGURE 13. Outlet Concentration Due to Re-Entrainment as a Function of Time

impurities was around 0.05 g/L. This concentration implies that the original scrubbing solution droplet entrained in the exit off gas would have to have been approximately 10 to 20 μm in diameter to result in an aerosol in the size range of the detector (0.3 to 0.7 μm) once the water had evaporated. Entrainment of droplets of this size is quite possible under the operating conditions of this study.

Influence of Scrubbing-Solution Concentration on Re-Entrainment. The influence of scrubbing-solution concentration on performance was investigated by adding either sodium chloride or titanium dioxide to the scrubbing solution while drawing room air through the SBS. The outlet concentration was monitored using the CSAS. One experiment was repeated using both sodium chloride and titanium dioxide to determine the difference between soluble and insoluble materials. The results are displayed in Figure 14.

The SBS was filled with fresh process water at the start of each experiment; yet the initial outlet concentration was approximately three times higher

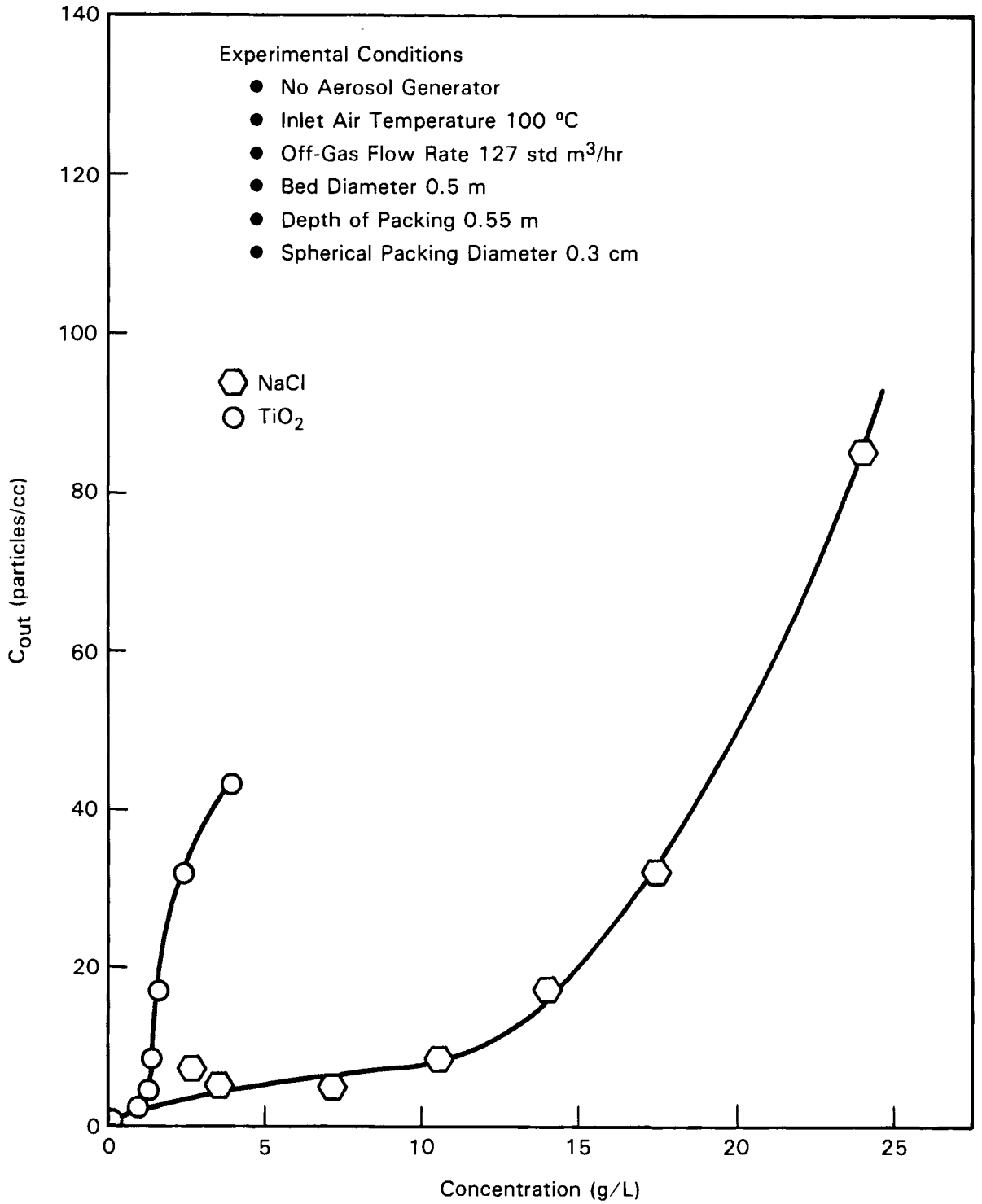


FIGURE 14. Effect of Scrubbing-Solution Concentration on Re-Entrainment

in the experiment with sodium chloride than in the experiment with titanium dioxide. The curves shown in Figure 14 have been corrected for this difference in initial concentrations, which are being considered background noise for the purposes of this study.

The curve for titanium dioxide climbs much more rapidly than the corresponding curve for sodium chloride. This behavior is consistent with the nature of the two chemical species. The titanium dioxide exists in the scrubbing solution as discrete particles, even at low concentrations. When a water droplet is entrained in the exit off gas, either there is a titanium dioxide particle in the droplet or there is not. If there is a particle, it should be large enough to be detected. This claim is based on the size distribution data for titanium dioxide suspended in the scrubbing solution, shown in Figure 15. Sodium chloride aerosols, on the other hand, will show a slower formation rate of 0.3- to 0.7-μm particles as its concentration increases in the scrubbing solution because it is distributed throughout the water as molecules, not as

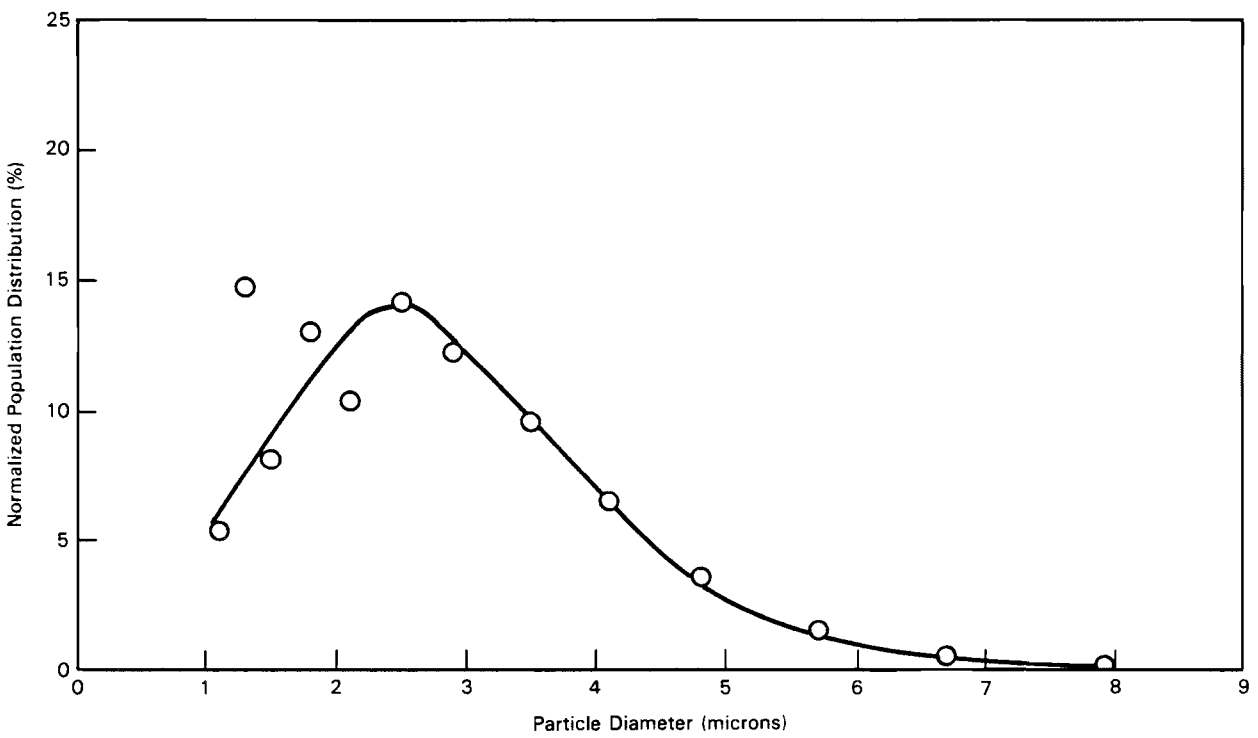


FIGURE 15. Particle Size Distribution of Titanium Dioxide Suspended in the Scrubbing Water (after adding ~36 kg $TiO_2$ to 650 L $H_2O$)

particles. The question of whether or not a "detectable" particle was formed depended on whether or not a titanium dioxide particle was present in the droplet in the first place. With sodium chloride, there will be material in the droplet, but the question is whether the droplet is large enough and/or the sodium chloride concentration high enough to produce a "detectable" particle once the water has evaporated. The number of droplets and the original size distribution produced are probably insensitive to the captured aerosol concentration on the scrubbing solution. However, the size distribution of sodium chloride aerosols generated after the water has evaporated will slowly shift towards larger particles as the concentration increases. Above a certain concentration, a significant portion of the resulting sodium chloride aerosols will be between 0.3 and 0.7 micron. This point appears to occur at a sodium chloride concentration in the scrubbing liquor of approximately 15 g/L.

There is a limit as to how much insoluble material can remain suspended in the scrubbing solution for a given rate of agitation. During the titanium dioxide experiment, the suspended-solids concentration only increased from 2.3 to 3.8 g/L as the amount of additional titanium dioxide increased from 16.2 to 36 kg. Better than 90% of the titanium dioxide did not remain suspended, suggesting that the suspended-solids concentrations investigated cover the range of concentrations likely to be encountered during long-term operation.

Influence of Velocity on Re-Entrainment. The off-gas velocity was varied at the end of the two previous experiments to determine the influence of velocity on re-entrainment. The results are shown in Figure 16. The curve for sodium chloride demonstrates an exponential-type increase with velocity, while the curve for titanium dioxide is closer to being linear. If the increase in the re-entrained aerosol concentration with velocity was merely a result of more droplets being formed, then both curves should exhibit the same shape. The fact that the curve for sodium chloride increases faster than the curve for titanium dioxide implies that the size distribution of the droplets formed by bursting bubbles increases towards larger particles at higher flow rates. The increased importance of re-entrainment at higher velocities is one of the reasons why scrubbing performance decreases with increasing velocity. For this reason, it is important to design an SBS such that the superficial velocities

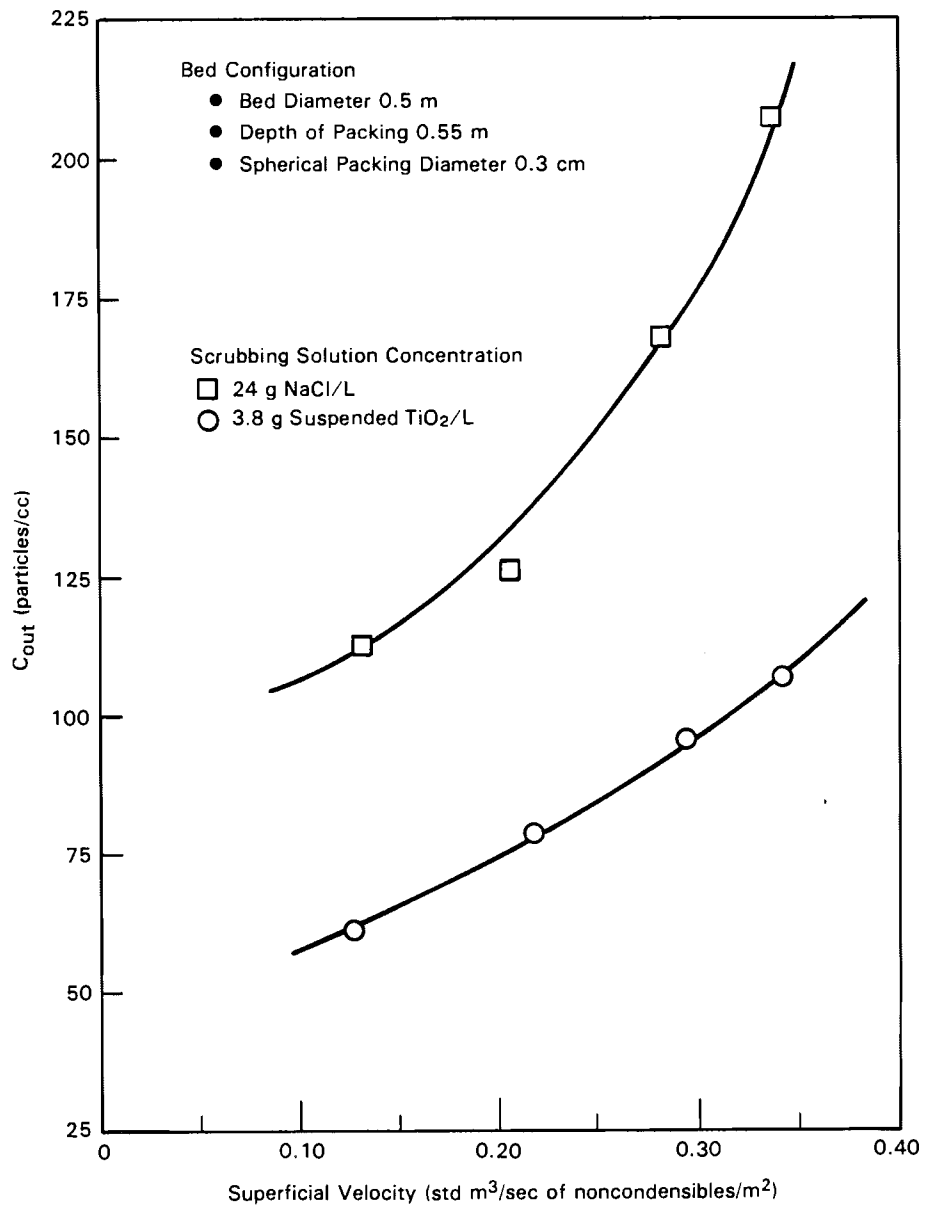


FIGURE 16. Effect of Gas Velocity on Re-Entrainment

are as low as reasonably possible. Lower flow rates also increase the effectiveness of the Brownian motion capture mechanism.

Influence of Defoamers on Re-Entrainment. Adding 36 kg of titanium dioxide to the scrubbing solution only increased the outlet concentration a little more than twice its level at the start of the experiment (before the correction for background noise was made). While these numbers may seem small, they

severely limit the performance of the SBS. At an inlet concentration of 1000 particles/cc, the mass DF is approximately 20 for insoluble aerosols at high aerosol concentrations in the scrubbing solution, assuming that all of the particles entering the SBS are initially captured. Any aerosols leaving as particles penetrating the SBS will lower the DF even more. As previously mentioned, the DF for soluble aerosols is almost always limited by re-entrainment. It is for this reason that efforts were directed to limit re-entrainment. One approach investigated was to lower the surface tension of the scrubbing solution, thus making it easier for the bubbles to break the surface of the scrubbing water. There should then be less potential energy stored in the gas within the bubble when it finally breaks, making it more difficult to form droplets that can become re-entrained. A defoamer supplied by Dow Corning (DB-110A) was added to the scrubbing solution after adding 16.2 kg of salt to the scrubbing solution. The effect of the defoamer on the outlet concentration is shown in Figure 17. After 50 grams (less than two ounces) was added to the approximately 650 liters of salt solution, the outlet concentration dropped below the background level observed at the start of the experiment. The addition of more defoamer did little to improve the outlet concentration.

A possible explanation has been extended as to the defoamer's effectiveness; but this hypothesis has not been proven, nor has the defoamer been tested under industrial conditions. It is sufficient to say that there does appear to be a practical way to limit re-entrainment, even for concentrated scrubbing solutions. It may also be possible to improve the initial capture of insoluble aerosols using a surfactant. The surfactant should increase the wettability of the insoluble material, making it easier for the aerosols to penetrate the gas-liquid interface (Goldshmid and Calvert 1963).

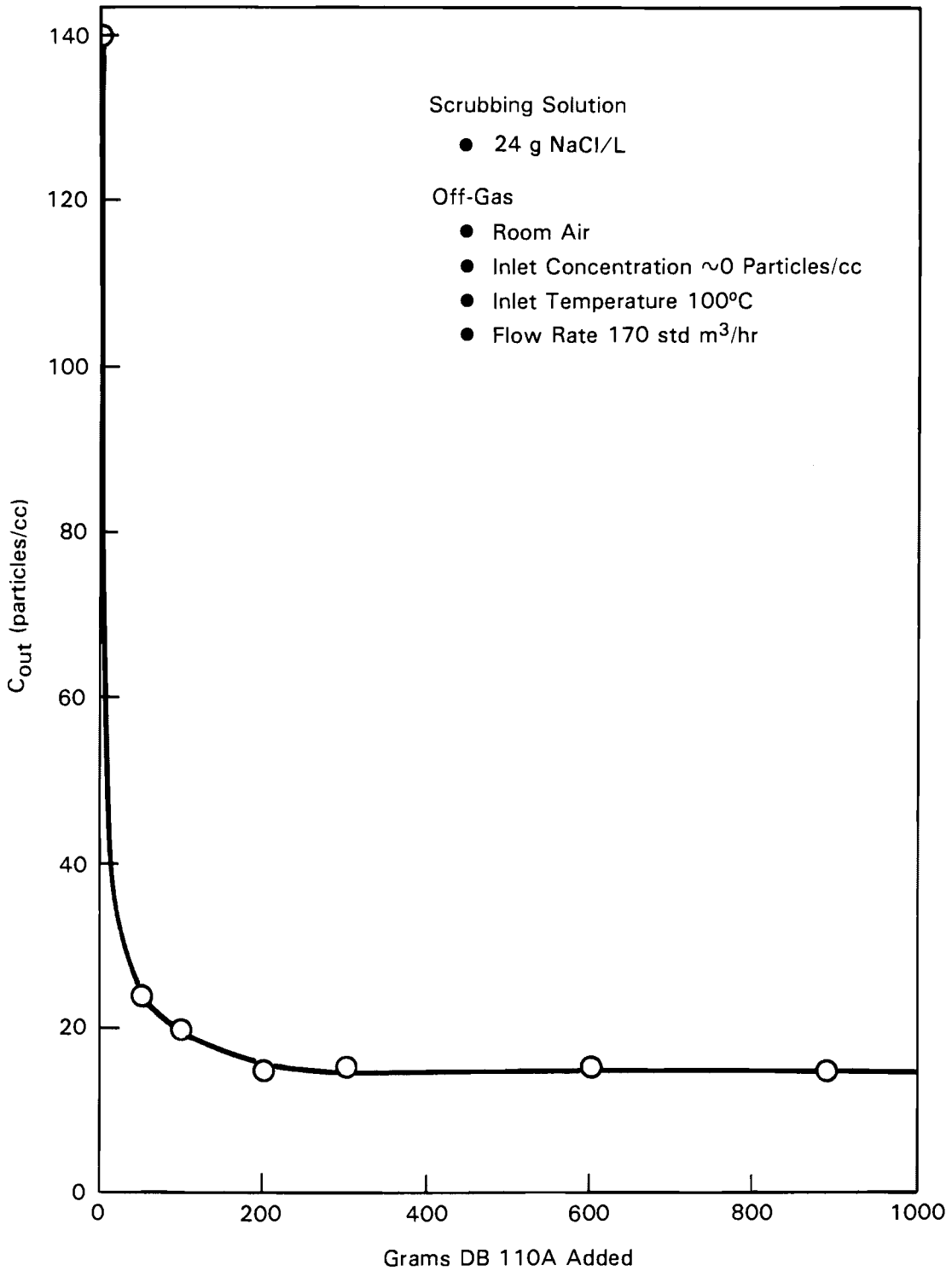


FIGURE 17. Effect of Dow Corning Defoamer DB-110A on Re-Entrainment

# 6.0 CONCLUSIONS AND RECOMMENDATIONS

The recently developed SBS has not, until now, undergone a rigorous scoping study to determine important operating ranges. The results of this study clearly demonstrate the importance of understanding SBS characteristics before designing one for a given application. Several parameters will affect the capture performance of the SBS. Many of these parameters were investigated in this study; their influence is summarized below. The expected influence of some of the parameters not studied is also addressed.

## 6.1 INFLUENCE OF INVESTIGATED PARAMETERS

The investigated parameters are divided into three categories: 1) process variables or inlet conditions, 2) dimensions and configuration of the SBS, and 3) operating parameters for the SBS.

### 6.1.1 Process Variables

The process variables or inlet conditions important to SBS performance include the off-gas flow rate, steam-to-air ratio, humidity, inlet concentration, and aerosol solubility.

- Superficial Velocity

  Increasing the superficial velocity will adversely affect the scrubbing performance by allowing less time for Brownian diffusion to occur, as well as resulting in increased re-entrainment. DFs for insoluble aerosols ranged from 7 to 12 at low superficial velocities to approximately 4 at higher values. It is also desirable to minimize the total flow of noncondensible gases in order to limit the size of the SBS. This point applies primarily to the nuclear waste processing industry, where floor space in a remote environment is extremely expensive.

- Steam-to-Air Ratio

  The presence of steam enhances DFs by shifting the effective aerosol size distribution towards larger particles, pre-wetting the aerosols and creating a draft (Stephan flow) towards the condensing surface.

It may be advisable to inject steam into the off gas to improve scrubbing performance. Increases in the DF up to 50% were observed for insoluble aerosols.

- Humidity

The inlet humidity determines the temperature at which the condensible vapors present in the off gas will condense. The scrubbing efficiency can be significantly improved if condensation occurs in the downcomer assembly. This condition forces the vapors to condense on the aerosols instead of the surface of the gas-liquid interface, as would occur if the off gas did not drop below its dew point until coming in contact with the scrubbing solution. Operating in this mode increased the DF from approximately 10 to approximately 40 for insoluble aerosols. In one case, the DF approached 60.

- Aerosol Solubility

There is a substantial difference in the ability of the SBS to remove aerosols, depending on the solubility of the material. The SBS appears capable of capturing nearly all soluble aerosols in the off gas, although a certain fraction of them eventually become re-entrained. Insoluble aerosols can penetrate the SBS more easily because of the difficulty associated with wetting the particles. As a particle hits the gas-liquid interface, it must be absorbed by the liquid. Soluble aerosols are easily captured by the liquid. The insoluble aerosols, on the other hand, are not captured as easily because of the difficulty in wetting the particle. The insoluble particle will not immediately penetrate the interface unless it hits the boundary with sufficient force. If the insoluble particles do not have enough momentum to penetrate the interface, they will rest on the surface before being adsorbed by the liquid. During this time they can become dislodged from the interface and re-enter the off gas. The addition of a surfactant may sufficiently decrease the resistance of the gas-liquid barrier and facilitate capture of insoluble aerosols by the scrubbing solution. Nominal DFs were approximately 100 for soluble aerosols and 10 for insoluble aerosols.

- Inlet Concentration

  For soluble aerosols, the outlet concentration is independent of the inlet concentration, suggesting that the removal of soluble aerosols from the off gas is re-entrainment limited. Thus, the DF increases quickly with inlet concentration for soluble aerosols. The insoluble aerosol scrubbing performance also appears to improve with inlet concentration. This occurrence is probably due to increased interactions between aerosols with increases in concentration, resulting in agglomerated particles that are easier to capture.

### 6.1.2 Design Variables

Design variables are the parameters that the engineer controls at the design stage of the SBS. The design variables investigated included the bed diameter and the packing size.

- Bed Diameter

  The bed diameter has an indirect influence on the scrubbing efficiency, because it determines the superficial velocity for a given off-gas flow rate. A larger bed diameter would result in longer residence times, allowing the aerosols more time to migrate from the bubble to the scrubbing solution and limiting re-entrainment. It is important to note that the effectiveness of the bed depends on uniform inlet gas distribution. Larger-diameter beds will require more carefully designed inlet gas distributors.

- Packing Size

  Experiments with 1-cm packing indicate an increase in performance over the 0.3-cm packing by approximately 10 to 20%. The increase in efficiency is probably due to the gas flow pattern through the bed. The void spaces within the 1-cm packing are sufficiently large for discrete bubbles to form and flow up through the packing. The void spaces in the smaller packing are not large enough for bubble formation; instead continuous gas phase channels form through the packing. Any increase in performance resulting from the increase in removal

efficiency by interception is overshadowed by the decrease in the residence time, which adversely affects the other predominant capture mechanism, Brownian motion.

### 6.1.3 Operating Variables

Because the SBS is a passive system, there are very few operating parameters. The only operating parameters that significantly influence the scrubbing performance involve the scrubbing solution. The operating parameters investigated included the scrubbing solution concentration and the addition of defoamers.

- Scrubbing Solution Concentration

  The scrubbing solution concentration and the off-gas velocity are important variables affecting the amount of material re-entrained. Re-entrainment increases with both concentration and gas velocity. The captured aerosol concentration in the scrubbing solution can be limited by injecting more steam into the off gas upstream of the SBS or by adding additional flush water to the reservoir. Either method will increase the purge rate.

- Defoamer

  A defoamer can be used to help eliminate re-entrainment. A commercially available defoamer was shown to essentially eliminate re-entrainment after 50 grams was added to the SBS containing sodium chloride in the scrubbing solution at a concentration of 24 g/L. More information is needed to determine the life of this defoamer under industrial conditions.

## 6.2 EXPECTED INFLUENCE OF SOME ADDITIONAL PARAMETERS

Other parameters will influence the aerosol scrubbing performance of the SBS, but were not studied. Some of these parameters were not investigated because they were only expected to have a minor effect on performance. In other cases, a particular parameter was not studied because its practical operating range was not large enough to have a major influence.

- Particle Size Distribution

  Only particles in the 0.3- to 0.7-micron size range were considered in this study, since this range typically represents the region of minimum scrubbing efficiency. Smaller particles are easily captured as a result of Brownian motion. These particles are so small that they easily diffuse off their streamlines, increasing the probability that they will migrate to a collecting surface. Larger particles are removed efficiently by impaction because they have too much inertia to follow their streamlines around obstacles. Still larger particles are subject to collection by settling. The particles in the 0.1- to 1.0-μm range are too large to be effectively influenced by Brownian diffusion and too small to have enough inertia for efficient removal by impaction. It is important to note that the DFs reported in this study are conservative in the sense that the actual mass DF will be higher for equivalent experimental conditions, when a larger particle size range is considered. Both the larger and the smaller particles will be removed more efficiently; thus, the DF as calculated on a mass basis will be significantly larger.

- Inlet Temperature (>200°C)

  The inlet temperature should affect the scrubbing performance once it is high enough that a significant radial temperature profile can be established inside a bubble. Thermophoresis will cause the aerosols in the bubble to migrate down the temperature gradient towards the gas-liquid interface. This phenomenon should increase the capture of aerosols. Higher inlet temperatures will allow for larger reductions in bubble size as the scrubbing solution cools the hot off gas. The shorter transport distances to the gas-liquid interface should result in higher removal efficiencies.

- Depth of Packing

  Increases in packing depth should always lead to increases in performance, unless the DF is already re-entrainment limited. Increasing the depth of packing in the SBS requires that an equivalent

pressure drop be incurred. This places practical limits on the depth of packing for off-gas systems operated under vacuum. Since the SBS may also be serving as a quencher, it may be that the water level is determined by that necessary to cool the off gas sufficiently and not by the amount of packing necessary to achieve the desired aerosol removal efficiency.

It is apparent from this study that the key to improving the performance of the SBS lies in improving the ability to make small bubbles to minimize transport distances, improving the ability of insoluble aerosols to penetrate the gas-liquid interface, and limiting the re-entrainment of material once it is captured. It is recommended that further tests be conducted to improve the performance of the SBS in these areas.

# 7.0 REFERENCES


Boucher, R. M. G. 1961. "Ultrasonics in Processing." Chem. Eng. 68(20):83.

Calvert, S., and H. M. Englund. 1984. Handbook of Air Pollution Technology. John Wiley and Sons, New York.

Calvert, S., and S. Gandhi. 1977. Fine Particle Collection by a Flux-Force/Condensation Scrubber: Pilot Demonstration. EPA-600/2-77-238, U.S. Environmental Protection Agency, Washington, D.C.

Calvert, S., and N. C. Jhaveri. 1974. "Flux Force/Condensation Scrubbing." J. Air Pollut. Control Assoc. 24(10):946.

Danser, H. W., and E. P. Neuman. 1949. "Industrial Sonic Agglomeration and Collection Systems." Ind. Eng. Chem. 41(11):2439.

Dean, J. A., ed.. 1973. Lange's Handbook of Chemistry, p. 458. McGraw-Hill, New York.

Devir, S. E. (Weinstock). 1967. "On the Coagulation of Aerosols III. Effect of Weak Electric Charges on Rate." J. Colloid. Interface Sci. 23(1):80.

Durham, M. D., and D. H. Lundgren. 1980. "Evaluation of Aerosol Aspiration Efficiency as a Function of Stokes Number, Velocity Ratio, and Nozzle Angle." J. Aerosol Sci. 11:179.

Fletcher, N. H. 1958. "Size Effect in Heterogeneous Nucleation." J. Chem. Phys. 29(3):572.

Friedlander, S. K. 1977. Smoke, Dust and Haze. John Wiley and Sons, New York.

Gillespie, T. 1953. "The Effect of the Electric Charge Distribution on the Aging of an Aerosol." Proc. R. Soc. London, Ser. A 216A:569.

Goldshmid, Y., and S. Calvert. 1963. "Small Particle Collection by Supported by Liquid Drops." AIChE J. 9:352.

Goles, R. W., and G. J. Sevigny. 1983. Off-Gas Characteristics of Defense Waste Vitrification Using Liquid-Fed Joule Heated Ceramic Melters. PNL-4819, Pacific Northwest Laboratory, Richland, Washington.

Green, H. L., and W. R. Lane. 1964. Particulate Clouds: Dust, Smokes, and Mists. 2nd Edition, Van Nostrand, New Jersey.

Gurley, R. N., K. M. LaRue, R. J. Thompson, K. R. Shah, J. E. Minor and D. H. Siemens. 1986. "Design Aspects of the Hanford Waste Vitrification Plant." In High Level Waste, Vol. 2 of Symposium on Waste Management at Tucson, Arizona, March 2-6, 1986, University of Arizona, Tucson, Arizona.

Hesketh, H. E. 1986. Fine Particles in Gaseous Media. Lewis Publishers, Inc., Chelsea, Michigan.

Hidy, G. M. 1984. Aerosols - An Industrial and Environmental Science. Academic Press, Inc., New York.

Hilliard, R. K., J. D. McCormack and A. K. Postma. 1981. Submerged Gravel Scrubber Demonstration as a Passive Air Cleaner for Containment Venting and Purging with Sodium Aerosols. HEDL-TME 81-30, Hanford Engineering Development Laboratory, Richland, Washington.

Hinds, W. C. 1982. Aerosol Technology: Properties, Behavior, and Measurement of Airborne Particles. John Wiley and Sons, New York.

Kitamura, M., M. Hatta, R. Tatsugae, T. Takeda, M. Hagiwara, N. Sasaki, H. Kashihara and M. Yamamoto. 1986. "Development of HLLW Vitrification Off-Gas Treatment Process in Japan." Presented at the American Nuclear Society Spectrum '86 International Topical Meeting, October 14-16, Niagara Falls, New York.

Liu, B. Y. H., D. Y. H. Pui, K. L. Rubow and W. W. Szymanski. 1985. "Electrostatic Effects in Aerosol Sampling and Filtration." Ann. Occup. Hyg. 29(2):251.

McCarthy, D., A. J. Yankel, R. G. Patterson and M. L. Jackson. 1976. "Multistage Fluidized Bed Collection of Aerosols." Ind. Eng. Chem., Process Des. Dev. 15(2):266.

Miller, R. C., and P. Kusch. 1956. "Molecular Composition of Alkali Halide Vapors." J. Chem. Phys. 25(5):860.

Ostle, B. O., and R. W. Mensing. 1982. Statistics in Research. The Iowa State University Press, Ames, Iowa.

Ruecker, C. M., and P. A. Scott. 1986. Design Procedure for Sizing a Submerged-Bed Scrubber for Airborne Particulate Removal. PNL-6036, Pacific Northwest Laboratory, Richland, Washington.

Saffman, P. G., and J. S. Turner. 1956. "On the Collision of Drops in Turbulent Clouds." J. Fluid Mech. 1:16.

Schifftner, K. C., and H. E. Hesketh. 1986. Wet Scrubbers. Lewis Publishers, Inc., Chelsea, Michigan.

Scott, P. S., R. W. Goles and R. D. Peters. 1985. Technology of Off-Gas Treatment for Liquid-Fed Ceramic Melters. PNL-5446, Pacific Northwest Laboratory, Richland, Washington.

Shaw, D. T. 1978. Recent Developments in Aerosol Science. John Wiley and Sons, New York.

Siemens, D. H., M. M. Beary, S. M. Barnes, D. N. Berger, R. A. Brouns, C. C. Chapman, R. M. Jones, R. D. Peters and M. E. Peterson. 1986. Design and Operating Features of the High-Level Waste Vitrification System for the West Valley Demonstration Project. PNL-5780, Pacific Northwest Laboratory, Richland, Washington.

St. Clair, H. W. 1949. "Agglomeration of Smoke, Fog, or Dust Particles by Sonic Waves." Ind. Eng. Chem. 41(11):2434.

Stokes, R. H., and R. A. Robinson. 1949. "Standard Solutions for Humidity Control at 25°C." Ind. Eng. Chem. 41:2013.

White, H. J. 1963. Industrial Electrostatic Precipitation. Addison-Wesley Publishing Company, Inc., Reading, Massachusetts.

# APPENDIX

TABLE A.1. 0.5-m-Diameter Bed with 1-cm Packing

| Run # | Inlet Aerosol Concentration (particles/cc) | Volumetric Flow Rates | | | Off-Gas Inlet T (°C) | Aerosol | Scrubbing Water T (°C) | Mass DF |
|---|---|---|---|---|---|---|---|---|
| | | Air (std $m^3$/h) | Steam (std $m^3$/h) | Ratio | | | | |
| 1 | 396 | 298 | 0 | 0 | 99.2 | NaCl | 20.6 | 2.8 |
| 2 | 1009 | 297 | 0 | 0 | 99.8 | NaCl | 20.0 | 26.3 |
| 3 | 1135 | 114 | 0 | 0 | 99.3 | NaCl | 19.5 | 127.2 |
| 4 | 1104 | 86 | 0 | 0 | 40.6 | $TiO_2$ | 21.4 | 4.5 |
| 5 | 1106 | 113 | 47.6 | 0.42 | 62.9 | $TiO_2$ | 19.7 | 39.9 |
| 6 | 1004 | 126 | 42.6 | 0.34 | 59.2 | $TiO_2$ | 20.3 | 58.8 |
| 7 | 1000 | 127 | 0 | 0 | 58.4 | $TiO_2$ | 19.1 | 4.2 |
| 8 | 751 | 213 | 0 | 0 | 57.5 | $TiO_2$ | 20.8 | 4.7 |
| 9 | 803 | 258 | 143 | 0.56 | 101.2 | $TiO_2$ | 25.7 | 2.3 |
| 10 | 803 | 262 | 142 | 0.54 | 100.5 | $TiO_2$ | 19.3 | 2.9 |
| 11 | 1095 | 215 | 0 | 0 | 62.1 | $TiO_2$ | 19.8 | 3.3 |
| 12 | 1073 | 209 | 97.7 | 0.34 | 58.0 | NaCl | 19.8 | 5.7 |
| 13 | 889 | 215 | 71.0 | 0.33 | 100.3 | NaCl | 19.7 | 21.4 |
| 14 | 1143 | 123 | 62.9 | 0.51 | 98.2 | NaCl | 19.8 | 611.5 |

0.55 m of packing, 0.172 $m^2$ cross-sectional area

TABLE A.2. 0.4-m-Diameter Bed with 1-cm Packing

| Run # | Inlet Aerosol Concentration (particles/cc) | Volumetric Flow Rates: Air (std $m^3/h$) | Volumetric Flow Rates: Steam (std $m^3/h$) | Volumetric Flow Rates: Ratio | Off-Gas Inlet T (°C) | Aerosol | Scrubbing Water T (°C) | Mass DF |
|---|---|---|---|---|---|---|---|---|
| 15 | 1035 | 171 | 0 | 0 | 62.4 | $TiO_2$ | 20.9 | 5.5 |
| 16 | 966 | 124 | 41.1 | 0.33 | 100.0 | $TiO_2$ | 19.9 | 6.9 |
| 17 | 1019 | 73 | 37.4 | 0.51 | 100.5 | $TiO_2$ | 19.9 | 8.5 |
| 18 | 832 | 173 | 56.2 | 0.32 | 99.8 | NaCl | 19.9 | 105 |
| 19 | 942 | 76 | 24.6 | 0.32 | 62.1 | NaCl | 20.2 | 81.2 |
| 20 | 951 | 123 | 60.6 | 0.49 | 64.8 | NaCl | 20.9 | 91.8 |
| 21 | 1171 | 172 | 59.1 | 0.34 | 100.5 | NaCl | 19.9 | 145 |

0.52 m of packing, 0.0995 $m^2$ cross-sectional area

TABLE A.3. 0.4-m-Diameter Bed with 0.3-cm Packing

| Run # | Inlet Aerosol Concentration (particles/cc) | Volumetric Flow Rates: Air (std $m^3$/h) | Volumetric Flow Rates: Steam (std $m^3$/h) | Volumetric Flow Rates: Ratio | Off-Gas Inlet T (°C) | Aerosol | Scrubbing Water T (°C) | Mass DF |
|---|---|---|---|---|---|---|---|---|
| 22 | 1289 | 72 | 0 | 0 | 100.4 | $TiO_2$ | 19.7 | 7.6 |
| 23 | 1138 | 73 | 0 | 0 | 100.9 | $TiO_2$ | 19.8 | 8.6 |
| 24 | 1151 | 121 | 41.4 | 0.34 | 59.4 | $TiO_2$ | 20.2 | 15.9 |
| 25 | 1254 | 168 | 57.2 | 0.34 | 101.7 | $TiO_2$ | 21.3 | 9.5 |
| 26 | 890 | 124 | 0 | 0 | 99.6 | NaCl | 19.6 | 64.1 |
| 27 | 1347 | 74 | 37.4 | 0.51 | 63.2 | NaCl | 20.8 | 49.0 |
| 28 | 1114 | 125 | 0 | 0 | 102.0 | NaCl | 19.7 | 37.6 |
| 29 | 833 | 179 | 85.0 | 0.47 | 58.4 | NaCl | 22.4 | 65.4 |

0.55 m of packing, 0.0995 $m^2$ cross-sectional area

TABLE A.4. 0.5-m-Diameter Bed with 0.3-cm Packing

| Run # | Inlet Aerosol Concentration (particles/cc) | Volumetric Flow Rates: Air (std $m^3$/h) | Volumetric Flow Rates: Steam (std $m^3$/h) | Volumetric Flow Rates: Ratio | Off-Gas Inlet T (°C) | Aerosol | Scrubbing Water T (°C) | Mass DF |
|---|---|---|---|---|---|---|---|---|
| 30 | 1055 | 130 | 0 | 0 | 59.6 | NaCl | 20.0 | 603 |
| 31 | 1136 | 127 | 43.3 | 0.34 | 102.4 | NaCl | 20.7 | 252 |
| 32 | 1165 | 217 | 71.5 | 0.34 | 58.8 | NaCl | 19.2 | 29.1 |
| 33 | 899 | 129 | 62.5 | 0.48 | 60.3 | $TiO_2$ | 19.5 | 43.2 |
| 34 | 1085 | 206 | 105 | 0.51 | 100.4 | $TiO_2$ | 19.2 | 5.4 |
| 35 | 908 | 215 | 104 | 0.48 | 100.5 | $TiO_2$ | 19.6 | 4.6 |
| 36 | 586 | 284 | 96.2 | 0.34 | 58.0 | $TiO_2$ | 18.6 | 4.1 |

0.55 m of packing (runs #30-32), 0.172 $m^2$ cross-sectional area
0.51 m of packing (runs #33-35)
0 m of packing (run #36)

TABLE A.5. 0.5-m-Diameter Bed with 1-cm Packing

| Run # | Inlet Aerosol Concentration (particles/cc) | Volumetric Flow Rates: Air (std $m^3$/h) | Volumetric Flow Rates: Steam (std $m^3$/h) | Volumetric Flow Rates: Ratio | Off-Gas Inlet T (°C) | Aerosol | Scrubbing Water T (°C) | Mass DF |
|---|---|---|---|---|---|---|---|---|
| 37 | 1116 | 125 | 0 | 0 | 100.0 | $TiO_2$ | 20.2 | 6.2 |
| 38 | 1116 | 124 | 61.5 | 0.50 | 101.3 | $TiO_2$ | 21.0 | 10.3 |
| 39 | 1116 | 124 | 43.3 | 0.35 | 101.1 | $TiO_2$ | 19.5 | 8.5 |
| 40 | 1243 | 207 | 0 | 0 | 100.9 | $TiO_2$ | 19.8 | 4.4 |
| 41 | 1243 | 206 | 69.8 | 0.34 | 101.1 | $TiO_2$ | 20.0 | 6.0 |
| 42 | 1243 | 204 | 105 | 0.52 | 100.0 | $TiO_2$ | 19.4 | 7.7 |
| 43 | 1091 | 89 | 0 | 0 | 103 | $TiO_2$ | 19.8 | 7.6 |
| 44 | 1091 | 88 | 43.2 | 0.49 | 101.1 | $TiO_2$ | 18.6 | 11.7 |
| 45 | 1091 | 88 | 28.9 | 0.33 | 98.5 | $TiO_2$ | 20.1 | 10.7 |
| 46 | 1108 | 181 | 0 | 0 | 99.1 | $TiO_2$ | 20.3 | 4.7 |
| 47 | 1314 | 181 | 0 | 0 | 102.0 | $TiO_2$ | 19.7 | 5.8 |
| 48 | 1314 | 176 | 56.9 | 0.32 | 101.1 | $TiO_2$ | 20.5 | 7.1 |
| 49 | 1314 | 177 | 88.3 | 0.50 | 101.8 | $TiO_2$ | 20.3 | 7.4 |
| 67 | 1011 | 297 | 0 | 0 | 100.6 | $TiO_2$ | 20.0 | 3.1 |
| 68 | 1010 | 284 | 96.0 | 0.34 | 99.9 | $TiO_2$ | 18.9 | 3.6 |
| 69 | 1011 | 284 | 145 | 0.51 | 100.1 | $TiO_2$ | 20.6 | 3.9 |
| 50 | 1116 | 127 | 0 | 0 | 101.0 | NaCl | 19.4 | 55.6 |
| 51 | 1116 | 125 | 42.8 | 0.34 | 99.2 | NaCl | 20.6 | 64.8 |
| 52 | 1116 | 124 | 61.3 | 0.49 | 100.9 | NaCl | 20.4 | 63.1 |
| 54 | 1131 | 216 | 0 | 0 | 99.6 | NaCl | 19.6 | 161 |
| 55 | 1131 | 210 | 69.8 | 0.33 | 101.2 | NaCl | 19.8 | 109 |
| 56 | 1131 | 206 | 104 | 0.50 | 100.1 | NaCl | 20.8 | 80.2 |

TABLE A.5. (contd)

| Run # | Inlet Aerosol Concentration (particles/cc) | Volumetric Flow Rates | | | Off-Gas Inlet T (°C) | Aerosol | Scrubbing Water T (°C) | Mass DF |
|---|---|---|---|---|---|---|---|---|
| | | Air (std $m^3$/h) | Steam (std $m^3$/h) | Ratio | | | | |
| 57 | 1187 | 86 | 0 | 0 | 99.4 | NaCl | 20.4 | 139 |
| 58 | 1187 | 84 | 27.9 | 0.33 | 100.0 | NaCl | 20.6 | 79.9 |
| 59 | 1187 | 84 | 42.3 | 0.50 | 100.0 | NaCl | 19.6 | 70.6 |
| 60 | 1020 | 172 | 0 | 0 | 99.2 | NaCl | 19.4 | 178 |
| 61 | 1387 | 166 | 85.3 | 0.51 | 99.8 | NaCl | 20.1 | 127 |
| 62 | 1387 | 166 | 55.9 | 0.34 | 100.8 | NaCl | 20.0 | 225 |
| 63 | 1083 | 298 | 0 | 0 | 102.0 | NaCl | 20.1 | 273 |
| 64 | 1083 | 273 | 141 | 0.52 | 101.5 | NaCl | 21.4 | 15.5 |
| 65 | 1083 | 277 | 97.5 | 0.35 | 99.4 | NaCl | 19.3 | 28.0 |
| 66 | 1123 | 129 | 0 | 0 | 59.7 | NaCl | 20.2 | 150 |
| 70 | 1045 | 297 | 0 | 0 | 64.3 | $TiO_2$ | 20.8 | 4.4 |
| 71 | 1172 | 284 | 95.6 | 0.34 | 58.3 | $TiO_2$ | 19.7 | 8.4 |
| 72 | 1122 | 176 | 0 | 0 | 60.8 | $TiO_2$ | 20.4 | 7.7 |
| 73 | 957 | 86 | 0 | 0 | 62.0 | $TiO_2$ | 20.8 | 7.8 |

0.55 m of packing, 0.172 $m^2$ cross-sectional area

TABLE A.6. 0.4-m-Diameter Bed with 1-cm Packing

| Run # | Inlet Aerosol Concentration (particles/cc) | Volumetric Flow Rates: Air (std $m^3/h$) | Volumetric Flow Rates: Steam (std $m^3/h$) | Volumetric Flow Rates: Ratio | Off-Gas Inlet T (°C) | Aerosol | Scrubbing Water T (°C) | Mass DF |
|---|---|---|---|---|---|---|---|---|
| 74 | 1011 | 78 | 0 | 0 | 62.4 | $TiO_2$ | 19.9 | 6.6 |
| 75 | 1009 | 74 | 0 | 0 | 60.0 | $TiO_2$ | 20.5 | 8.5 |
| 76 | 1079 | 127 | 0 | 0 | 100.3 | $TiO_2$ | 19.6 | 8.0 |
| 77 | 940 | 126 | 61.7 | 0.49 | 64.0 | $TiO_2$ | 20.3 | 43.3 |
| 78 | 1079 | 49 | 0 | 0 | 99.9 | $TiO_2$ | 20.7 | 8.7 |
| 79 | 1006 | 71 | 26.7 | 0.38 | 100.9 | $TiO_2$ | 20.4 | 9.0 |
| 80 | 1118 | 100 | 0 | 0 | 98.8 | $TiO_2$ | 19.9 | 9.1 |
| 81 | 1071 | 71 | 0 | 0 | 99.0 | $TiO_2$ | 19.9 | 9.2 |
| 82 | 1094 | 53 | 0 | 0 | 100.4 | $TiO_2$ | 20.3 | 8.5 |
| 83 | 1075 | 175 | 0 | 0 | 99.6 | $TiO_2$ | 19.8 | 5.3 |
| 84 | 1058 | 48 | 0 | 0 | 98.5 | NaCl | 20.6 | 29.1 |
| 85 | 2034 | 48 | 0 | 0 | 100.4 | NaCl | 20.5 | 53.6 |
| 86 | 553 | 51 | 0 | 0 | 100.6 | NaCl | 19.6 | 20.0 |
| 87 | 2695 | 52 | 0 | 0 | 100.3 | NaCl | 19.6 | 90.2 |

0.55 m of packing, 0.0995 $m^2$ cross-sectional area

TABLE A.7. 0.4-m-Diameter Bed with 0.3-cm Packing

| Run # | Inlet Aerosol Concentration (particles/cc) | Volumetric Flow Rates | | | Off-Gas Inlet T (°C) | Aerosol | Scrubbing Water T (°C) | Mass DF |
|---|---|---|---|---|---|---|---|---|
| | | Air (std $m^3$/h) | Steam (std $m^3$/h) | Ratio | | | | |
| 88 | 1041 | 79 | 0 | 0 | 101.6 | $TiO_2$ | 20.2 | 7.1 |
| 89 | 1139 | 50 | 0 | 0 | 99.8 | $TiO_2$ | 19.6 | 8.5 |
| 90 | 1058 | 124 | 0 | 0 | 100.0 | $TiO_2$ | 20.4 | 5.6 |
| 91 | 1074 | 100 | 0 | 0 | 100.0 | $TiO_2$ | 20.2 | 6.6 |
| 92 | 1079 | 172 | 0 | 0 | 99.8 | $TiO_2$ | 20.8 | 6.1 |
| 94 | 1042 | 74 | 37.0 | 0.50 | 100.5 | $TiO_2$ | 21.6 | 4.2 |
| 95 | 1198 | 80 | 0 | 0 | 99.4 | $TiO_2$ | 19.6 | 7.4 |

0.55 m of packing, 0.0995 $m^2$ cross-sectional area

TABLE A.8. 0.5-m-Diameter Bed with 0.3-cm Packing

| Run # | Inlet Aerosol Concentration (particles/cc) | Volumetric Flow Rates: Air (std $m^3$/h) | Volumetric Flow Rates: Steam (std $m^3$/h) | Volumetric Flow Rates: Ratio | Off-Gas Inlet T (°C) | Aerosol | Scrubbing Water T (°C) | Mass DF |
|---|---|---|---|---|---|---|---|---|
| 98 | 1110 | 132 | 0 | 0 | 101.6 | $TiO_2$ | 20.2 | 5.0 |
| 99 | 1095 | 92 | 0 | 0 | 100.8 | $TiO_2$ | 20.6 | 6.1 |
| 100 | 1069 | 215 | 0 | 0 | 100.3 | $TiO_2$ | 20.2 | 3.4 |
| 101 | 1036 | 169 | 0 | 0 | 99.8 | $TiO_2$ | 20.0 | 4.6 |
| 102 | 1048 | 126 | 0 | 0 | 60.2 | $TiO_2$ | 19.9 | 5.6 |
| 103 | 1088 | 93 | 0 | 0 | 60.7 | $TiO_2$ | 19.8 | 5.2 |
| 104 | 1096 | 174 | 0 | 0 | 59.9 | $TiO_2$ | 20.1 | 4.5 |
| 105 | 1122 | 208 | 0 | 0 | 60.2 | $TiO_2$ | 20.4 | 3.4 |
| 106 | 1110 | 285 | 0 | 0 | 58.8 | $TiO_2$ | 20.1 | 2.5 |
| 107 | 1039 | 282 | 0 | 0 | 100.8 | $TiO_2$ | 20.4 | 2.8 |
| 108 | 1097 | 124 | 0 | 0 | 99.3 | NaCl | 20.5 | 26.7 |
| 109 | 1056 | 128 | 0 | 0 | 99.9 | CsCl | 20.6 | 20.0 |
| 110 | 1092 | 130 | 0 | 0 | 99.9 | $CsNO_3$ | 20.8 | 18.4 |
| 111 | 1088 | 131 | 0 | 0 | 99.4 | $TiO_2$ | 21.0 | 5.6 |
| 112 | 787 | 126 | 0 | 0 | 99.6 | $RuO_2$ | 20.5 | 3.9 |

0.55 m of packing (runs #98-105)
0.36 m of packing (runs #106-112)

# DISTRIBUTION

No. of Copies

OFFSITE

30 DOE Technical Information Center

6 DOE Office of Civilian Radioactive Waste Management
Forrestal Building
Washington, DC 20585
ATTN: C. R. Cooley, RW-4
J. R. Hilley, RW-30
S. Kale, RW-20
D. E. Shelor
R. Stein, RW-23
L. H. Barrett, RW-33

3 DOE Office of Defense Waste & Transportation Management
GTN
Washington, DC 20545
ATTN: G. H. Daly, DP-124
J. E. Lytle, DP-12
T. C. Chee, DP-123

5 DOE Office of Remedial Action and Waste Technology
GTN
Washington, DC 20545
ATTN: J. A. Coleman, NE-24
T. W. McIntosh, NE-24
W. R. Voigt, NE-20
H. F. Walter, NE-24
J. B. Zorn, NE-25

A. T. Clark
Division of Fuel Material Safety
Nuclear Regulatory Commission
Washington, DC 20555

No. of Copies

V. Stello
Office of the Executive Director for Operations
Mail Station 6209
Nuclear Regulatory Commission
Washington, DC 20555

G. L. Sjoblom
Environmental Protection Agency
Office of Radiation Programs
401 M Street, S.W.
Washington, DC 20460

J. M. McGough
DOE Albuquerque Operations Office
P.O. Box 5400
Albuquerque, NM 87185

P. G. Hagan
Joint Integration Office
Bldg. 3, 2nd Floor
2201 San Pedro N.E.
Albuquerque, NM 87110

E. Maestas
DOE West Valley Operations Office
P.O. Box 191
West Valley, NY 14171

2 DOE Idaho Operations Office
550 Second Street
Idaho Falls, ID 83401
ATTN: S. T. Hinschberger
J. P. Hamric

F. T. Fong
DOE San Francisco Operations
1333 Broadway
Oakland, CA 94612

No. of
Copies

M. R. Jugan
DOE Oak Ridge Operations Office
P.O. Box E
Oak Ridge, TN 37830

W. J. Brumley
DOE Savannah River Operations Office
P.O. Box A
Aiken, SC 29801

M. J. Steindler
Argonne National Laboratory
9700 South Cass Avenue
Argonne, IL 60439

C. S. Abrams
Argonne National Laboratory
P.O. Box 2528
Idaho Falls, ID 83401

3 Battelle Memorial Institute
Project Management Division
505 King Avenue
Columbus, OH 43201
ATTN: W. A. Carbeiner
W. S. Madia
Technical Library

L. D. Ramspott
Lawrence Livermore National Laboratory
University of California
P.O. Box 808
Livermore, CA 94550

D. T. Oakley, MS 671
Los Alamos Scientific Laboratory
P.O. Box 1663
Los Alamos, NM 87544

No. of
Copies

4 Oak Ridge National Laboratory
P.O. Box Y
Oak Ridge, TN 37830
ATTN: J. O. Blomeke
W. D. Burch
R. T. Jubin
L. J. Mezga

Sandia Laboratories
P.O. Box 5800
Albuquerque, NM 87185
ATTN: Technical Library

J. R. Berreth
Westinghouse Idaho Nuclear Co., Inc.
P.O. Box 4000
Idaho Falls, ID 83401

7 E. I. du Pont de Nemours Company
Savannah River Laboratory
Aiken, SC 29801
ATTN: R. G. Baxter
M. D. Boersma
J. G. Glasscock
F. M. Heckendorn
J. R. Knight
M. J. Plodinec
C. T. Randall

E. A. Jennrich
EG&G Idaho
P.O. Box 1625
Idaho Falls, ID 83415

R. Shaw
Electric Power Research Institute
3412 Hillview Avenue
P.O. Box 10412
Palo Alto, CA 94304

No. of
Copies

5 West Valley Nuclear Services Company
P.O. Box 191
West Valley, NY 14171
ATTN: S. M. Barnes
C. C. Chapman
J. E. Krauss
S. J. Marchette
J. M. Pope

J. L. White
Energy Research & Development Authority
Empire State Plaza
Albany, NY 12223

A. K. Postma
Rt. 1, Box 46A
Halfway, OR 97834

ONSITE

9 DOE Richland Operations Office

J. H. Anttonen
E. A. Bracken
G. J. Bracken
C. E. Collantes
C. R. DeLannoy
J. M. Peterson
J. L. Rhoades
M. W. Shupe
J. D. White

9 Rockwell Hanford Operations

T. D. Anderson
J. M. Henderson
R. D. Prosser
J. L. Scott
D. A. Turner
D. D. Wodrich
R. D. Wojtasek
B. D. Wolfe
File Copy

No. of
Copies

UNC United Nuclear Industries

T. E. Dabrowski/W. J. Kyriazia

2 Westinghouse Hanford Company

R. E. Lerch
J. D. Watrous

51 Pacific Northwest Laboratory

C. R. Allen
W. W. Ballard, Jr.
W. F. Bonner
R. A. Brouns (2)
J. L. Buelt
H. C. Burkholder
J. R. Carrell
R. D. Dierks
L. J. Ethridge
R. W. Goles
L. K. Holton
S. S. Koegler
W. L. Kuhn
L. T. Lakey (2)
D. E. Larson
S. F. Liebetrau
J. L. McElroy
J. E. Minor
R. K. Nakaoka
J. M. Perez, Jr.
R. D. Peters
M. E. Peterson
C. M. Ruecker (10)
P. A. Scott (5)
G. J. Sevigny
S. C. Slate
J. E. Surma
N. M. Thomas
J. H. Westsik, Jr.
Publishing Coordination (2)
Technical Report Files (5)